1703 Pigmented Hepatocellular Neoplasms Have a High Risk for Atypia and Malignancy

Saba Yasir, Taofic Mounajjed, Michael Torbenson. Mayo Clinic, Rochester, MN.

Background: Pigment deposition is occasionally seen in hepatocellular neoplasms (HN), some of which are densely pigmented and called pigmented hepatic adenoma (HA). Several case reports suggest that pigmented HA has an increased risk for malignancy, but pigmented HNs remain poorly studied.

Design: 108 well-differentiated HNs diagnosed or submitted for consultation as HA or atypical HA, were retrospectively reviewed for pigment deposition; 26 (24%) had pigment identified within hepatocytes at 10x magnification. Pigmented HNs were stained for iron and reticulin, and immunostains for liver fatty acid binding protein (LFABP), β-catenin, gluthamine synthesase (GS), C-reactive protein (CRP), serum amyloid A (SAA), glypican3 (GPC3), and ki67. A subset was evaluated by electron microscopy (EM).

Results: All cases were negative for iron and EM confirmed the pigment was lipofuschin. Lipofuschin showed intense granular staining with GPC3 in 23 (88%) cases, but no diffuse cytoplasmic staining was seen. 11 cases were classified as HA (42%), 6 as HN of uncertain malignant potential (HUMP) (23%), and 9 as hepatocellular carcinoma (HCC) (35%). Of the 9 HCCs, 4 arose in a pigmented HA (overall rate of malignant transformation in pigmented HA: 27%). Most patients (21, 81%) were female, but males (5, 19%) only had HCC (4) or HUMP (1). The average age at diagnosis was 38 years. Tumors averaged 8.1 cm in size. 10 patients (38%) had multiple HNs (2 to >50). Other HNs were not pigmented in 9/10 (90%) of patients with multiple HNs, but only the pigmented HNs had atypia or malignancy, leading to a diagnosis of HUMP or HCC in 4 of the 9 patients. By immunophenotype, HNs were HNF1α inactivated in 13 (50%) cases (8 HA, 4 HUMP, and 1 HCC), β-catenin activated in 7 (27%) cases (6 HCC and 1 HUMP), inflammatory in 3 (12%) cases (2 HA and 1 HUMP), concurrently β-catenin activated and inflammatory in 1 HA, concurrently HNF-1α inactivated and β-catenin activated in 1 HA, and unclassified in 1 HCC. Ki67 was <1% in 24 (92%) cases, and increased in 2 cases (1 HUMP and 1 HCC).

Conclusions: Phenotypically, pigmented HNs represent a heterogenous group, with HNF-1α inactivation being the commonest phenotype. However, pigmented HNs have an increased risk of atypia and malignancy, with most classified as HUMP or HCC. In fact, even cases classified as HA had a high risk (27%) of malignant transformation. The increased risk of malignancy is further indicated by the fact that only pigmented HNs had atypia or malignancy in patients with multiple pigmented and non-pigmented HNs. Male gender is especially associated with malignancy.

1704 Alterations in Degree of Steatosis of Liver Allografts

Yang Zhang, William Twaddell. University of Maryland, Baltimore, MD.

Background: Liver transplantation for patients with acute liver failure and end-stage liver disease has increased in recent years. The demand for donor livers is increasing and organ shortage has become a significant problem. In response, institutions across the United States have started adopting less stringent guidelines regarding which donor livers they will accept. Steatosis in the donor liver has been extensively studied as a potential prognostic factor for success and outcomes of liver transplantation, with macrovesicular steatosis > 30% associated with worse outcomes. However, steatosis remains a relative contraindication rather than an absolute contraindication, and increasingly steatotic livers are being used in transplantation.

Steatosis is likewise a common finding in assessment of liver allografts for dysfunction. In the current study, we aim to investigate how the degree of steatosis in the liver allograft changes in the immediate post-operative period. By looking at how long it takes a liver allograft to lose its fat in its new host environment, we hope to understand when the histologic finding of steatosis indicates pathology in the host rather than the donor.

Design: We selected cases of orthotopic liver transplantation with multiple biopsies of the liver allograft, which included remarks by the pathologist on the degree of steatosis, and evaluated the degree of steatosis at different time points. Data were analyzed using 1-tailed t-tests.

Results: In patients showing an eventual decrease in liver fat content, such changes happened rapidly. Specimens from this group taken within one week of transplantation had a mean of 52% steatosis, while specimens taken two weeks or more following transplantation showed a mean of 7% steatosis ($p = 0.0005$). In patients showing an eventual increase in steatosis a similar change was seen: within one week of transplantation, biopsy showed a mean of 7% steatosis, while after two weeks the mean was 45%. In this case, the value was not statistically significant, probably due to the small number of cases analyzed.

Conclusions: These results indicate that fat content in a donor liver changes precipitously within the first two weeks following transplant. This occurred in patients with an eventual decrease as well as those with an eventual increase in the level of liver allograft steatosis. The findings suggest that beyond the initial two weeks following orthotopic liver transplantation, steatosis seen in the allograft liver most likely represents pathology in the host rather than pathology in the donor.

1705 Histopathologic Features Related To Progression of Fibrosis in Sequential Biopsies in Non-Alcoholic Steatohepatitis (NASH)

Lei Zhao, Rish Pai, Won-Tak Choi, Qin Shao, Maria Westerhoff, Zu-Hua Gao, John Hart. University of Chicago, Chicago, IL; University of Washington, Seattle, WA; Cleveland Clinic, Cleveland, OH; McGill University, Montreal, QC, Canada.

Background: The goal of this study is to identify histologic features in NASH biopsies useful in predicting progression of fibrosis.

Design: 51 NASH patients who underwent 2 biopsies ³1 year apart were studied. Histologic features (ballooning, Mallory bodies, lobular & portal inflammation, lobular neutrophils, steatosis & fibrosis stage) were scored in initial biopsies. Centrilobular zone (CLZ) CK7+ elements were quantitated by form (scattered single cells, string of cells, or ductules) and degree (mild or florid) in initial biopsies (CK7 & glutamine synthetase immunostains performed). Portal ductular reaction (PDR) was scored as mild or florid. Fibrosis stage (NIDDK system) was scored for follow-up biopsies.

Results: The mean interval between biopsies was 2.5 years (range 1.0-7.5). Fibrosis stage progressed in 51%, was stable in 33%, & regressed in 16%. Histologic features of hepatocellular injury in NASH all correlated with current fibrosis stage, however, none predicted fibrosis progression.

Histologic Features in Initial Biopsy	Fibrosis Stage in Initial Biopsy		Progression of Fibrosis	
	Rs	P Value	Rs	P Value
Steatosis	0.26	0.03	-0.14	0.16
Lobular Inflammation	0.36	0.004	0.11	0.23
Neutrophils	0.31	0.01	0.01	0.46
Ballooning	0.44	0.0006	0.004	0.49
Mallory Bodies	0.44	0.0007	-0.05	0.36
Portal Inflammation	0.31	0.01	0.03	0.42

CLZ CK7+ elements also demonstrated high correlation with current fibrosis stage. Furthermore, florid CLZ CK7+ elements showed positive correlation with fibrosis progression(p=0.06).

CK7+ Elements/DR in Initial Biopsy	Fibrosis Stage in Initial Biopsy		Progression of Fibrosis	
	Rs	P Value	Rs	P Value
CLZ Single Cells	0.13	0.19	-0.11	0.22
CLZ Strings	0.54	0.00002	0.01	0.46
CLZ Ductules	0.54	0.00003	0.17	0.11
CLZ mild CK7	0.28	0.02	-0.14	0.16
CLZ florid CK7	0.52	0.00004	0.21	0.06
PDR mild	-0.06	0.32	-0.18	0.1
PDR florid	0.31	0.01	-0.08	0.28

Conclusions: This study confirms that histologic features of hepatocellular damage in NASH are associated with fibrosis, but these features are not predictive of fibrosis progression. In contrast, florid CLZ CK7+ elements appear to be a histologic feature useful to predict fibrosis progression.

Neuropathology and Ophthalmic Pathology

1706 Genomic Alterations in Skull Base Meningiomas

Malak Abedalthagafi, Wenya Linda Bi, Yu Mei, Brian Alexander, Rameen Beroukhim, Ossama Al-Mefty, Ian Dunn, Azra Ligon, Sandro Santagata. Brigham & Women's Hospital, Boston, MA; Dana-Farber Cancer Institute and Harvard Medical School, Boston, MA.

Background: The genomic underpinnings of meningiomas remains incompletely understood, despite their prevalence in adults. We prospectively analyzed the genomic profiles of a large cohort of skull base meningiomas and assessed relevant pathological and clinical variables.

Design: Copy-number-alterations (CNAs) were analyzed using high-resolution array-based comparative genomic hybridization. Factors associated with outcome were assessed.

Results: 140 skull base meningiomas from 139 patients (78F/61M, mean age 55 yrs, range 22-90 yrs) were profiled. The majority of tumors were de novo, 37 were recurrent, and 7 patients harbored multiple intracranial meningiomas. 59 tumors had prior radiation exposure, 28 being radiation-induced,and 31 patients having received post-operative adjuvant radiation. The most common tumor locations were petroclival/petrosal (25), sphenoid wing (13), parasagittal/falcine (28), planum sphenoidale/olfactory groove (10), and tuberculum/clinoid (9), followed by intraventricular, middle fossa, tentorial, torcular, cavernous sinus, and foramen magnum locations. 82 were WHO grade I (38 meningothelial, 13 fibroblastic, 17 transitional, 4 secretory, 4 angiomatous, 2 psammomatous); 51 were grade II (42 atypical, 7 chordoid, 2 clear cell); and 7 were grade III (6 anaplastic, 1 rhabdoid). 18 tumors exhibited brain invasion and 37 had intratumoral necrosis. Monosomy 22 was the most frequent copy-number alteration, occurring in 56%. Frequently observed alterations included: loss of chromosome 1p (all:41%, grI:10%, gr II:78%, grIII:83%); 6q (all:22%, grI:5%, grII:50%, grIII:100%); 7p (all:15%, grI:0%, grII:33%, gr III:83%); 10q (all:10%, grI:2%, grII:22%, grIII:33%); and 18q (all:16%, grI:3%, grII:33%, grIII:83%). The incidence of chromosomal loss varied significantly by location. Meningiomas involving the sagittal sinus, torcula, and cavernous sinus harbored the highest rate of CNAs (1p-:65%; 6q-:29%; 18q-:29%; monosomy 22:76%). Petrosal/petroclival and sphenoid meningiomas also expressed higher CNAs than planum sphenoidale/olfactory and tuberculum/clinoid meningiomas. Polysomy involving multiple chromosomes characterized angiomatous meningiomas.

Conclusions: Traditional histopathologic classifications fail to fully account for the natural history and growth patterns of intracranial meningiomas. Systematic genomic characterization of a large series of skull base meningiomas reveal distinct subsets of tumors, which may be further correlated with clinical outcomes.

1707 The SNP-CN Microarray Shows High Concordance and Greater Sensitivity in Detecting Molecular Alterations Compared To FISH and SNaPshot

Christina Appin, Stewart Neill, Matthew Schniederjan, Stephen Hunter, Debra Saxe, Charles Hill, Michael Rossi, Daniel Brat. Emory University School of Medicine, Atlanta, GA.

Background: Infiltrating gliomas comprise approximately 30% of all primary intracranial tumors. These tumors are widely infiltrative and therefore incurable, with the vast majority progressing to higher grade neoplasms. Molecular studies such as fluorescence in situ hybridization (FISH), somatic mutation panels and single nucleotide polymorphism (SNP)-copy number (CN) microarrays, reveal diagnostically and prognostically important alterations in the routine workup of diffuse gliomas. SNP-CN microarrays assess abnormalities across the entire genome, providing information on copy number abnormalities, allelic imbalances, loss of heterozygosity, deletions, amplification events and some somatic mutations. The purpose of this study was to determine how closely the molecular alterations seen by SNP-CN microarray correlate with those seen by FISH and a SNaPshot mutation panel.

Design: The SNP-CN microarray was performed at our institution on 55 infiltrating gliomas, including 33 glioblastomas (GBMs), 13 astrocytomas (grade 2 and 3) and 9 oligodendrogliomas (grade 2 and 3). Of these, FISH for *EGFR* amplification, *PTEN* deletion and/or 1p/19q co-deletion was done on 48 gliomas and the SNaPshot mutation panel was performed on 37 gliomas. Molecular diagnostics and cytogenetics reports were compared to determine correlations among these 3 tests.

Results: In 44 cases, the SNP-CN microarray identified all alterations detected by FISH. However, in 4 cases the SNP-CN microarray revealed loss of chromosome 10 (including *PTEN*) that was not detected by FISH (91.7% concordance). Both SNaPshot and the SNP-CN microarray detected the same point mutations in 15 cases, including 14 *IDH1* mutations (R132H) and one *BRAF* mutation (V600E). No point mutations were identified in 22 cases by either SNaPshot or the SNP-CN microarray. However, in one case, the SNP-CN microarray identified one *IDH1* mutation (R132H) that was not detected by SNaPshot (97.3% concordance). In this case, the tumor showed immunoreactivity for the IDH1 mutant protein antibody (R132H).

Conclusions: The SNP-CN microarray results show high concordance with FISH and SNaPshot mutation testing. Additionally, this test shows greater sensitivity in detecting molecular alterations than FISH or SNaPshot.

1708 Analyses of LIN28A Expression and C19MC Amplification in Malignant Pediatric CNS Tumors

Asuka Araki, Moninka Chocholous, Thomas Czech, Karin Dieckmann, Daniela Prayer, Irene Slavc, Christine Haberler. Medical University of Vienna, Vienna, Austria.

Background: CNS-PNETs are rare highly malignant CNS tumors, comprising CNS PNETs NOS, (ganglio)neuroblastoma, ependymoblastoma (EBL) and medulloepithelioma (MEP). Furthermore, a new highly aggressive entity designated as embryonal tumor with abundant neuropil and true rosettes (ETANTR) has been described. ETANTR is characterized by amplification of a microRNA cluster located in chromosome 19q13.42 (*C19MC)* and by immunohistochemical cytoplasmic expression of LIN28A. Recently, *C19MC* amplification and LIN28A expression has been also described in EBL and MEP, suggesting that ETANTR, MEP and EBL comprise a distinct entity. However, LIN28A expression has been found also in other malignant brain tumors. Furthermore, single ETANTRs with LIN28A expression but without *C19MC* amplification have been reported. To extend the knowledge on these 2 markers, we examined a series of malignant pediatric brain tumors.

Design: 64 malignant pediatric brain tumors were examined by immunohistochemistry for Lin28A and FISH, using custom-made probes for the *C19MC* locus: 6 ETANTRs, 2 MEP and 2 EPB, as well as 8 CNS-PNETs, 9 medulloblastomas (MB), 7 malignant gliomas and 29 anaplastic ependymomas (AEP), which arise as differential diagnosis of ETANTR, EBL and MEP.

Results: All tumors originally diagnosed as ETANTR, MEP and EPB (n=10) showed cytoplasmic LIN28A expression. 7/10 tumors also harbored the *C19MC* amplification. Furthermore, 2 AEP, 2 MBs and 2 PNETs displayed LIN28A immunoreactivity, but had no *C19MC* amplification.

Conclusions: LIN28A expression is an important diagnostic marker to detect ETANTR, EBL and MEP, which are highly aggressive CNS tumors, but needs to be evaluated in the context of the histopathological tumor features.

1709 Immunohistochemistry Stain and Molecular Genetic Study of Hemangioblastoma: An Indication of Anti-VEGF Target Therapy

Sabina Babayeva, Banumathy Gowrishankar, Yang Wang, George Kleinman, John Abrahams, Bo Xu, Jane Houldsworth, Minghao Zhong. New York Medical College at Westchester Medical Center, Valhalla, NY; Cancer Genetics, Inc., Rutherford, NJ; Roswell Park Cancer Institute, Buffalo, NY.

Background: Hemangioblastomas (HB) are uncommon, slow-growing tumors of the central nervous system without available target therapy. Hemangioblastomas occur both sporadically and as an important component of von Hippel-Lindau (VHL) disease which is associated with clear cell RCC (ccRCC). Acutely, HB and ccRCC have some similarities at morphological level. Here, we would like to investigate sporadic HB by IHC stains and molecular genetic approach to explore the possibility of anti-VEGF target therapy which is suitable for ccRCC.

Design: 25 cases of sporadic HB were collected. For IHC stains, tissue microarray (TMA) was constructed. IHC stains of Pax8, CA9 and inhibin were applied to TMA slides. The UroGenRA™-Kidney Array-CGH Assay was used to evaluate molecular genetic changes in HB. This assay detects genomic alterations associated with the four main renal tumor subtypes: including loss of the Von Hippel-Lindau (VHL) gene in ccRCC.

Results: IHC stains have been applied to 25cases. All 25 cases of HB showed strongly, diffuse membrane stain of CA9 (identical to ccRCC); completely negative for Pax8 (renal marker). Only 10 cases were positive for inhibin. For the 10 cases of HB which undergo UroGenRATM-Kidney Array-CGH assay, 7 cases were found chromosome 3 deletion; 3 cases had chromosome 6 deletion; 2 cases presented no genetic change.

Conclusions: Our study demonstrated that hemangioblastoma are strongly positive for CA9 which is identical to that in ccRCC and indicates dysregulation of VHL-pseudohypoxia signal pathway. In addition, 70% of HB had chromosome 3 deletion. These results suggest that some cases of HB had gentic change similar to that of ccRCC and HB would be suitable of anti-VEGF target therapy. However, we could identify loss of VHL gene in 30% of HB cases. This indicates that those HB may use other molecular mechanism for down regulation of VHL gene, such as point mutations or promoter region hypermethylation which warrant for further study.

1710 Neuropathological Correlates of Periventricular Infarcts

Gayathiri Balasubramaniam, Joel Ramirez, Alicia McNeely, Fuqiang Gao, Courtney Berezuk, Christopher Scott, Sandra Black, Julia Keith. Sunnybrook Health Sciences Centre, University of Toronto, Toronto, ON, Canada.

Background: Collagenosis of periventricular veins may play a role in periventricular subcortical hyperintensities (pvSH) seen on MRI. When pvSH become large and confluent periventricular venous infarction (PVI) may occur. This study characterized the histological nature of PVIs using MRIs to guide sampling.

Design: MRIs were reviewed to identify subjects with PVIs. Using MRI images as a guide, PVIs were localized in formalin-fixed, coronally-sectioned cadaveric brain tissue, blocked and stained with H&E/LFB, Masson's trichrome, and immunohistochemistry for GFAP, CD68, and neurofilament. Slides were examined for 1. histological confirmation of an infarct, and 2. the presence and extent of venous collagenosis using a semi-qualitative scale of 0-3 for small (20 μm) and medium calibre (50-150μm diameter) veins, and collagenosis of large calibre periventricular veins was scored as % stenosis on trichrome staining.

Results: Based on MRI 6 subjects were enrolled with a total of 14 PVIs. Histological analysis characterized these PVIs as infarcts (N=4), enlarged perivascular spaces (N=3), or no detectable lesion (N=7). Based on gross observations of the cadaveric brain tissue the PVIs were dichotomized into grossly visible at autopsy versus grossly invisible at autopsy. Within the grossly visible PVI group 3 were infarcts and 2 were enlarged perivascular spaces. The average rating for small veins, medium veins and % stenosis in large veins for subjects with PVIs on imaging was 1.6, 0.92 and 31.1%. Small vein collagenosis was significantly more severe for histologically confirmed infarcts (M=2.25, SD=1.5) than non-infarcts (M=0.7, SD=0.95) (t(12)=2.7, p=0.036). The % stenosis of large calibre veins was greater for histologically confirmed infarcts (M=25.4, SD=8.9) than non-infarcts (M=16.4, SD=6.5) (t(11)=2.08, p=0.062).The % stenosis of large veins in the grossly visible at autopsy group (M=34.2, SD=7.4) was significantly greater than the grossly invisible at autopsy group (M=18.3, SD=9.2) (t(11)=3.02, p=0.01).

Conclusions: Collagenosis of both small and large calibre veins is a frequent finding in patients with PVIs on MRI and is especially common when infarction is histologically confirmed.

1711 Overexpression of the Chromatin Remodeling Proteins ARID1A, BRG1 and SMARCD3 in Adult and Pediatric Gliomas

Leomar Ballester, Zengfeng Wang, Markku Miettinen, Fausto Rodriguez, Eric Raabe, Javad Nazarian, Charles Eberhart, Katherine Warren, Martha Quezado. National Institutes of Health – National Cancer Institute, Bethesda, MD; Johns Hopkins Hospital, Baltimore, MD; Childrens Research Institute, Washington, DC.

Background: Brain tumors are the most common solid tumors in children. In particular, diffuse intrinsic pontine gliomas (DIPGs) are aggressive tumors with poor prognosis that account for 10-25% of pediatric brain tumors. In adults, gliomas are the most common malignant brain tumors, and usually carry a poor prognosis. In recent years, there has been a significant increase in the understanding of molecular defects of gliomas and multiple lines of evidence suggest a role for global epigenetic alterations in gliomagenesis. Mutations in chromatin remodeling complex genes are being recognized in many cancer types. However, very little is known about the potential contribution of chromatin remodeling proteins to the development of adult and pediatric gliomas. The SWI/SNF ATP-dependent chromatin-remodeling complex plays an essential role in a variety of cellular processes including differentiation, proliferation and DNA repair.

Design: Samples from 24 pediatric gliomas and 38 adult gliomas were included in the study. H&E stained slides were reviewed for confirmation of diagnosis by a neuropathologist. Cases included 24 DIPGs (autopsy material), and 38 adult gliomas: 10 low grade astrocytomas, 8 oligodendrogliomas, 4 ependymomas and 16 glioblastomas (GBMs). We used immunohistochemistry to assess the expression of various members of the SWI/SNF complex (ARID1A, BRG-1 and SMARCD3), as well as the transcription factor SATB1, in 62 gliomas.

Results: Our data shows that although normal glial cells are negative for ARID1A, BRG-1 and SMARCD3, these proteins are overexpressed in adult and pediatric gliomas. In contrast, SATB1 expression was not detected in the majority of cases. Specifically, our results showed that 11/22 (50%), 22/24 (92%) and 18/24 (75%) of DIPGs overexpressed ARID1A, BRG-1 and SMARCD3, respectively. Adult astrocytomas also overexpressed ARID1A 8/10 (80%), BRG-1 9/10 (90%) and SMARCD3 10/10 (100%), respectively. Oligodendrogliomas showed overexpression of BRG-1 (7/8, 88%), ARID1A (7/8, 88%) and SMARCD3 (8/8, 100%). Evaluation of 4 ependymomas also demonstrated overexpression of ARID1A (3/4, 75%), BRG-1 (4/4, 100%) and SMARCD3 (4/4, 100%), respectively.

Conclusions: Our study provides evidence for dysregulation of chromatin remodeling proteins (ARID1A, BRG-1 and SMARCD3) in adult and pediatric gliomas, although the underlying mechanism and consequences of the increased expression of these proteins remains to be elucidated.

1712 MDM2 Upregulation: A Novel Molecular Marker in Meningioma

Yalda Behbahanian, William Yong, Harry Vinters, Negar Khanlou. University of California, Los Angeles, CA.

Background: Meningiomas are commonly amenable to surgical resection and radiation therapy. However, their recurrence and malignant potential remain a challenge. Although morphology and proliferative rate (Ki67 index) are used routinely at clinical level to predict their aggressive behavior, the role of molecular factors, is not entirely determined. Recent studies have identified deregulations of p14–MDM2–p53 pathway as a contributory factor to the malignant progression of meningioma. However these were mainly tested on low grade tumors and few lesions evolving from low grade background. We investigated *MDM2* expression in low grade and anaplastic meningiomas using immunohistochemistry and established correlation with tumor grade and proliferative rate.

Design: 10 cases each of low grade (WHO grade I) and anaplastic meningiomas (WHO grade III) were selected from UCLA pathology archives. The latter group included 8 de novo malignant tumors and 2 evolving from atypical meningioma. Morphological review were performed and Ki67 index were obtained. MDM2 immunostain protocol was then performed on formalin-fixed paraffin-embedded tissue on all cases.

Results: MDM2 nuclear immunoreactivity and labeling index was determined using a semi-quantitative assessment. Cases were classified into four categories accordingly (score 1-4). Tumors showing no, or less than 5 percent MDM2 expression were considered negative (score 1). The remaining of the cases were tumors with 5-10% (score 2), 10-25% (score 3), and tumors with >25% nuclear labeling (score 4). Grade I meningiomas were predominantly score 1 (9/10 accounting for 90% of low grade cases). Only 1 low grade tumor expressed 5-10% nuclear staining (score 2). Contrastingly, high labeling index was observed in 8/10 of the de novo anaplastic meningiomas (80%), ranging from 10-25% (score 3) in 5/8 cases and >25% (score 4) in 3/8 cases. The remaining 2 anaplastic tumors showed 5-10% nuclear positivity (score 2) and were tumors evolving from atypical meningioma. MDM2 labeling index showed no significant correlation with Ki67 index (P value <0.0001).

Conclusions: In our study, elevated MDM2 was associated with aggressive meningiomas (Grade 2 and 3). Potential utility as an adjunct for grading and its prognostic value should be further studied. The presence of elevated MDM2 suggests the potential for targeted therapeutic intervention. The possibility for diagnostic utility will require comparative studies in meningioma mimics.

1713 Discordance Rates in Healing/Healed Arteritis in Temporal Artery Biopsies: The Role for Bilateral Biopsies

Paula Blanco, Danah Albreiki, Sangsu Han, James Farmer. University of Ottawa, The Ottawa Hospital, Ottawa, ON, Canada.

Background: Temporal artery biopsy (TAB) is the gold standard diagnostic modality for giant cell arteritis (GCA). Since bilateral positivity for active GCA is reported to be higher than 90%, unilateral TAB is considered standard of care for the investigation of GCA. However, GCA can present with active, healing/healed and no injury in a segmental, uneven distribution along the extracranial carotid artery tree. Healing/healed arterial injury in the proper clinical setting is usually treated as active GCA, and therefore identifying those cases become crucial. We studied the discordance rate (positive on one side and negative on the other side) for healing/healed arterial injury in bilateral TAB to verify whether unilateral biopsies would render as high a diagnostic yield as they do in active GCA.

Design: We retrospectively studied TAB performed by the same neuroophthalmologist at our institution in a 4 year period. We classified them into 3 categories: negative, healing/healed arterial injury, and active GCA. We defined healing/healed arterial injury as fibromyxoid intimal change, fragmentation and/or loss of the internal elastic lamina and medial scarring, with or without neovascularization. Focal areas of persistent chronic inflammation may remain. Statistical analysis was used to compare diagnostic sensitivity between both groups.

Results: Of the 257 TAB studied, 166 were negative, 56 were positive for active GCA and 35 showed healing/healed arterial injury. Fifty two of the active GCA cases (52/56) and 34 of the healing/healed arterial injury cases (34/35) had bilateral TAB performed. A bilateral positive result was observed in 46/52 (88%) of active GCA cases, while 6/52 (12%) cases showed unilateral positivity. Healing/healed arterial injury was identified bilaterally in 11/34 (32%) cases, while unilateral lesions were observed in 23/34 (68%) cases. Thirty four of the 35 cases (97%) with healing/healed arterial injury had high clinical suspicion and were treated as active GCA. The diagnostic sensitivity of unilateral TAB is significantly ($p<0.01$) lower for healing/healed arterial injury compared to active GCA.

Conclusions: Bilateral temporal artery biopsies should be the standard of care to detect the characteristic histopathological features of healing/healed arterial injury.

1714 BRAF-V600E Immunohistochemistry in a Large Series of Low Grade Glial and Glial-Neuronal Tumors of the Central Nervous System

Quentin Breton, Helene Plouhinec, Delphine Prunier-Mirebeau, Blandine Boisselier, Sophie Michalak, Philippe Menei, Audrey Rousseau. University Hospital of Angers, Angers, France.

Background: Neuronal-glial and neuronal tumors of the central nervous system (CNS) are rare WHO grade I or II neoplasms arising in children and young adults. Pilocytic astrocytoma (PA), a circumscribed WHO grade I glial tumor, may be difficult to distinguish from neuronal-glial tumors. BRAF is an oncogene frequently mutated (BRAF-V600E mutation) in melanomas and other cancers. The BRAF-V600E mutation has recently been identified in glial and glial-neuronal CNS tumors, such as pleomorphic xanthoastrocytomas (PXA), gangliogliomas (GG), and dysembryoplastic neuroepithelial tumors (DNET). Conversely, the mutation is rare in PA, especially in the cerebellum. Patients with BRAF-V600E-mutated tumors are eligible to targeted therapy, hence the relevance of detecting BRAF mutations in those CNS neoplasms. BRAF mutations can be detected by Sanger sequencing or reverse transcriptase PCR (RT-PCR), among others. A specific anti-BRAF-V600E antibody is now commercially available. It is known to be sensitive and specific to detect BRAF-V600E mutation in melanomas but it has not been widely studied in large series of glial and glial-neuronal tumors.

Design: The present study aimed at assessing anti-BRAF-V600E immunohistochemistry (IHC) compared to the gold standard (i.e. molecular biology techniques) in glial and glial-neuronal CNS tumors. 175 cases from 140 patients were retrospectively evaluated by anti-BRAF IHC and when possible, by Sanger sequencing and RT-PCR.

Results: By IHC, BRAF-V600E expression was detected in 40/140 patients (28.5%). 61% GG (32/53 cases), 44% PXA (4/9 cases), 5% PA (3/58 cases, all 3 supratentorial) and 0% DNET (0/6) were immunopositive. In 61% GG (22/36 cases), expression was present only in the ganglion cells and in 39% GG (14/36 cases), it was detected in both glial and neuronal components. 13/40 cases (32.5%) displayed BRAF-V600E mutation by sequencing. In our series, sensitivity and specificity of IHC were respectively 100% and 78%. In 4 cases with BRAF expression only in the (often rare) ganglion cells within the tumor, IHC was more sensitive than sequencing to detect the mutation.

Conclusions: IHC may add to the gold standard and should probably be performed even if genetic testing is ordered. Detecting the mutation in a few ganglion cells questions the potential efficacy (or at least, the mechanism of action) of targeted therapy in cases where wild type-BRAF glial tumor cells largerly overrun the neuronal component.

1715 Comprehensive Genomic Profiling of Brain Glioblastoma Reveals Frequent Clinically Relevant Genomic Alterations

Zachary Chalmers, Siraj Ali, Julia Elvin, Doron Lipson, Kai Wang, Roman Yelensky, Juliann Chmielecki, Alex Fichtenholz, Garrett Frampton, Vincent Miller, Philip Stephens, Jeffrey Ross. Foundation Medicine Inc, Cambridge, MA.

Background: Glioblastoma (GBM) are the highest grade malignant tumors of glial origin, typically with a predominantly astrocytic histology, and which commonly recur after initial surgical management. Evidence to guide treatment of progressive disease is lacking, and we queried whether comprehensive genomic profiling (CGP) of GBM cases would uncover clinically relevant genomic alterations (CRGA) that could lead to the rational use of targeted therapies for these challenging cases.

Design: DNA was extracted from 40 microns of FFPE sections from 576 GBM. CGP was performed on hybridization-captured, adaptor ligation based libraries to a mean coverage depth of 654X for 3,769 exons of 236 cancer-related genes plus 47 introns from 19 genes frequently rearranged in cancer. The results were evaluated for all classes of genomic alterations (GA) including base substitutions, short insertions and deletions, copy number changes and fusions/rearrangements. CRGA were defined as GA linked to drugs on the market or under evaluation in mechanism driven clinical trials.

Results: There were 362 male and 214 female patients with a mean age of 58 years (range 13-84 years). DNA was extracted from surgically biopsied or resected GBM cases as FFPE samples and submitted for CGP. CGP revealed 3,093 total GA (5.4 GA/sample), and 570 (99%) of GBM featured at least 1 CRGA with a total of 2,004 CRGA identified (3.5 CRGA/tumor). The most frequent CRGA were: *CDKN2A* (340), *EGFR* (232), *PTEN* (225), *NF1* (112), *EGFR-EGFR* truncation (106), *CDK4* (89), *PIK3CA* (81), *ATRX* (67), *IDH1* (64), *MDM2* (57), and *BRAF* (14 V600E substitutions and 10 other GA). Frequent GA identified included *CDKN2B* (299), *TP53* (225), *RB1*, (58), and *MDM4* (29). *BRAF* GA frequently co-occurred with *CDKN2A* deletion (18 of 24 *BRAF*+ cases). A triad of GA in *IDH1*, *TP53*, and *ATRX* is observed in 45 cases, with the remaining cases harboring either *ATRX* or *IDH1* alterations also often harboring *TP53* alterations. Clinical responses to targeted therapies will be presented.

Conclusions: GBM features a high frequency of CRGA detectable by CGP, and a subset of these malignancies can be defined by the co-occurrence of *IDH1*, *TP53*, and *ATRX*. These characterizations may further expand on known prognostic groupings within GBM, and could suggest the rational use of targeted therapies to improve clinical outcomes.

1716 Combinatorial Targeting of ATF5 and the PI3K/mTOR Signaling Pathway as a Therapeutic Strategy for Glioblastoma

Lily Chau, Georg Karpel-Massler, Chang Shu, James Angelastro, Lloyd Greene, Markus Siegelin. Columbia University, New York, NY; UC Davis School of Veterinary Medicine, Davis, CA.

Background: Glioblastoma multiforme (GBM), the most common adult primary brain tumor, is highly malignant with poor prognosis (median survival is 13-15 months). Response to therapy is limited owing to molecular heterogeneity and compensatory/parallel survival mechanisms.

Activating transcription factor 5 (ATF5) is highly expressed in human GBM samples and cell lines. Inhibition of ATF5 function results in apoptosis in vitro and clearance

of experimentally induced gliomas in vivo. The PI3K/Akt/mTOR signaling pathway - essential for proliferation, metabolism, and survival - is commonly activated in GBM and important for tumor growth and progression.
As such, combinatorial targeting of ATF5 and the PI3K/Akt/mTOR axis is an attractive therapeutic strategy. To target ATF5 and the PI3K signaling pathway, we used an ATF5 dominant-negative peptide (CP-d/n-ATF5) and NVP-BEZ235, a dual PI3K/mTOR inhibitor, respectively. Dual PI3K/mTOR inhibitors are particularly effective because they can short circuit the mTOR inhibition-induced negative feedback loop that results in PI3K/Akt activation.
Design: Human GBM cell lines T98G and LN229 were obtained from ATCC. Cells treated with CP-d/n-ATF5 and/or NVP-BEZ235 were labeled with annexin V-FITC/PI, then analyzed for cell viability and apoptosis using a BD FACSCalibur. Protein levels were analyzed by western blotting using antibodies for: mTOR, phospho mTOR, Akt, phospho Akt-Ser473, caspase 9, cleaved caspase 3, Mcl-1, Bcl-2, Bcl-xl, actin.
Results: CP-d/n-ATF5 and NVP-BEZ235 synergistically promote GBM cell apoptosis. At concentrations at which CP-d/n-ATF5 or NVP-BEZ235 alone have modest effects, combination treatment synergistically decreases cell viability and enhances apoptosis. CP-d/n-ATF5 alone results in decreased caspase 9 and increased cleaved caspase 3 protein levels; this effect is enhanced in combination treatment with NVP-BEZ235.
CP-d/n-ATF5 and NVP-BEZ235 mediate apoptosis via downregulation of anti-apoptotic Bcl-2 family proteins. CP-d/n-ATF5 alone results in decreased protein levels of Mcl-1, Bcl-2, and Bcl-xl; this effect is enhanced in combination with NVP-BEZ235.
Conclusions: CP-d/n-ATF5 and NVP-BEZ235 synergistically promote apoptotic cell death at least in part through downregulation of anti-apoptotic Bcl-2 family members. The dual targeting of ATF5 and PI3K/mTOR signaling is a promising novel therapeutic strategy for GBM. Future directions include investigating the anti-tumor efficacy of this drug combination in vivo.

1717 A Wide Spectrum of EGFR Mutations in Glioblastoma Is Detected By a Single Clinical Oncology Targeted Next-Generation Sequencing Panel

Patrick Cimino, Haley Abel, Eric Duncavage. Washington University School of Medicine, St. Louis, MO.

Background: With the advent of large scale genomic analysis, the genetic landscape of Glioblastoma (GBM) has become more clear, including characteristic genetic alterations in *EGFR*. In routine clinical practice, genetic alterations in GBMs are identified using several techniques including PCR, immunohistochemistry, sequencing, and fluorescence *in situ* hybridization (FISH) studies. Unfortunately, these disparate tests consume already limited amounts of tissue and add to overall testing costs. In this study, we focused on *EGFR* as a model gene in order to determine the spectrum of mutations that can be readily detected from next-generation sequencing (NGS) reads obtained from a targeted clinical oncology panel.
Design: We identified 34 GBMs, that were sequentially analyzed by a targeted NGS clinical oncology panel containing 151 genes, including *EGFR*, using DNA obtained from FFPE tissue. Single nucleotide variants (SNVs) were called using a standard pipeline while *EGFR* amplifications were called using CopyCat2. Concurrent confirmatory FISH and multiplex ligation dependent probe amplification (MLPA) was performed where there was sufficient remaining material.
Results: Twenty one of the 34 (62%) individuals had had at least one alteration in *EGFR* by sequencing, consistent with published datasets. Various SNVs were identified in *EGFR* including 10 non-synonymous mutations, 9 polymorphisms, 1 silent mutation, and 1 truncating mutation. *EGFR* amplification was identified in 20 (59%) individuals. Of those 20 cases, 15 (75%) were called positive for *EGFR* amplification by FISH, 4 were considered negative for *EGFR* amplification all of which had low level amplification by sequencing, and 1 case was equivocal for *EGFR* amplification by FISH. Three cases with *EGFR* amplification also were found to harbor the *EGFR*vIII mutation (confirmed by MLPA in samples with sufficient tissue) and 1 additional case had the *EGFR*vV mutation.
Conclusions: Here we show a single NGS assay can identify the full spectrum of clinically relevant mutations in *EGFR*, including amplification and *EGFR*vIII. This analysis could further extend to include other diagnostic, prognostic, and predictive genes of interest. Overall, sequencing based diagnostics have the potential to maximize the amount of genetic information obtained from GBMs and simultaneously reduce the total time, required specimen material, and costs associated with multimodality studies.

1718 Frequency of ATRX Mutations in Adolescent Mixed Oligoastrocytomas

Patrick Cimino, Katherine Schwetye, Robert Schmidt, Sonika Dahiya. Washington University School of Medicine, St. Louis, MO.

Background: While diffuse gliomas are relatively quite common in adult population, they are less prevalent in pediatric and adolescent age-group. The most well-known molecular marker for diffuse oligodendroglial neoplasms is the presence of co-deletions of chromosomes 1p and 19q. However, these genetic alterations largely apply to adult tumors as they are nearly absent in pediatric population and have a very low frequency in adolescents. More recently, α-thalassemia/mental retardation syndrome X-linked (ATRX) genetic mutations (with consequent loss of its protein expression) have been shown to to be mutually exclusive to 1p and 19q co-deletions in adult mixed oligoastrocytoma (MOA) series. With ATRX emerging as a marker for sub-stratification in adult MOAs, the adolescent population (aged 10-21 years) is relatively understudied and is in need of investigation.
Design: A search of our institutional files revealed a total of 22 MOA cases occurring in adolescent patients aged 10 to 20 years. Chart review was performed to obtain demographics and pertinent clinical information, such as 1p and 19 co-deletions. Of these 22 patients, 16 had additional material to be used for immunohistochemistry (IHC). IHC was performed using an anti-ATRX antibody (Sigma-Aldrich, 1:300 dilution) utilizing a Benchmark Ultra instrument (Ventana Medical Systems Inc.).
Results: The mean patient age was 17.5 years. While a majority of these (15/22; 68%) were WHO Grade II, the remaining were anaplastic (WHO grade III). ATRX nuclear staining was retained in 9/16 (56%) cases, lost in 6/16 (38%) cases, and equivocal in 1/16 (6%) case. Of the 9 cases with retained ATRX staining, only 1/9 (11%) was positive for 1p and 19q co-deletions. None of the 6 cases with lost ATRX staining, or the case of equivocal ATRX staining, had 1p and 19q co-deletions.
Conclusions: In our relatively small series of adolescent MOAs, 56% of cases showed retained expression of ATRX. Unlike adult MOAs that have a reported high correlation of ATRX retention with 1p and 19q co-deletions, this frequency is quite low in our small series of adolescent MOA cases.

1719 Comparative Immunohistochemical Expression of β-Catenin, EGFR, ErbB2, and p63 in Adamantinomatous and Papillary Craniopharyngiomas

Ghada Esheba, Amal Hassan. Faculty of Medicine, Umm AlQura University, Mecca, Saudi Arabia; Faculty of Medicine, Tanta University, Tanta, Egypt; Al Noor Hospital, Mecca, Saudi Arabia; Faculty of Medicine, Al-Azhar University, Cairo, Egypt.

Background: Craniopharyngiomas (CPs) are rare epithelial tumor located mainly in the sellar/parasellar region. CPs have been classified into histopathologically, genetically, clinically and prognostically two distinctive subtypes: adamantinomatous and papillary variants.
Design: To determine the immunohistochemical expression of β-catenin, EGFR, ErbB2, and p63 in adamantinomatous and papillary CPs.
β-catenin, EGFR1,ErbB 2, and p63 immunostaining was performed on paraffin embedded tissue sections of 25 CPs including 18 ACPs and 7 PCPs.
Results: 17 out of 18 cases (94%) of ACP exhibited strong nuclear/cytoplasmic expression of β-catenin. On the contrary, all cases of PCP showed exclusively membranous expression (P value < 0.0001). Regarding EGFR family, 15 (83%) and 5 cases (71%) of APC and PCP respectively were positive for EGFR1, while only 3 cases (17%) of APC and none of PCP had score 3+ for ErbB2. P63 over-expression was observed in 16 out of 18 ACP (89%) and 6 out of 7 PCP (86%).

Immunohistochemicalmarker	ACP (18 cases)	PCP (7 cases)
	No. of positive cases (%)	
β-catenin	17 (94%)	0
EGFR	15 (83%)	5 (71%)
ErbB2	3 (17%)	0
P63	16 (89%)	6 (86%).

However, the distribution of p63 staining was diffuse in ACP, where it stained the nuclei of basal layer cells and the whorl-like areas. While in PCP, p63 positivity was mainly restricted to the basal cell layer.

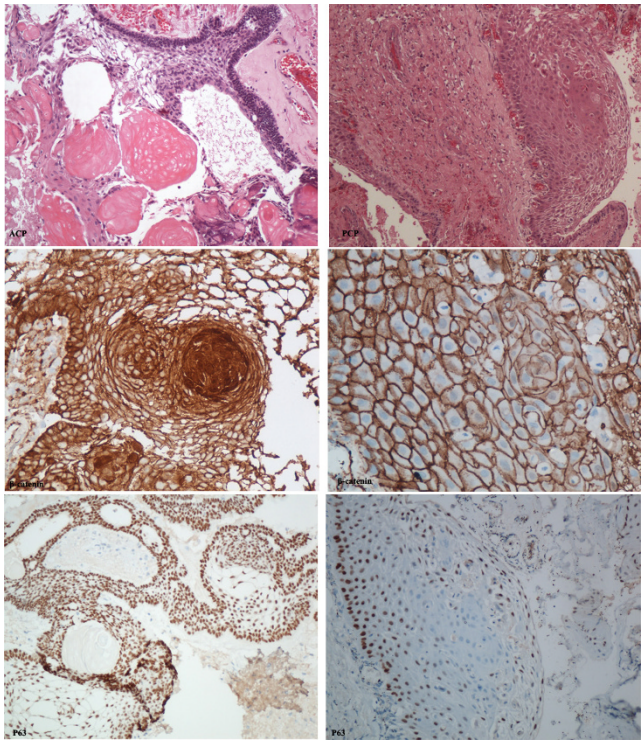

Conclusions: Nuclear accumulation of β-catenin is a diagnostic hallmark of the ACP, differentiating it from the PCP and is very helpful in the differential diagnosis between both subtypes in the setting of small biopsies. EGFR positivity in most cases of ACP

and PCP could qualify the use of anti- EGFR therapy. P63 over-expression in both ACP and PCP validates the possible role of 63 in maintaining the proliferative activity of the tumor cells and potentiate its important role in tumorigenesis.

1720 NAB2-STAT6 Gene Fusion in Meningeal Hemangiopericytoma and Solitary Fibrous Tumor

Karen Fritchie, Long Jin, Brian Rubin, Peter Burger, Andre Oliveira, Caterina Giannini. Mayo Clinic, Rochester, MN; Johns Hopkins University, Baltimore, MD; Cleveland Clinic, Cleveland, OH.

Background: While hemangiopericytoma (HPC) of soft tissue has been subsumed under the designation of solitary fibrous tumor (SFT), in the WHO Classification of CNS tumors (2007), HPC of the meninges remained a tumor entity with aggressive clinical behavior distinct from SFT. Recent work, however, has shown that many meningeal HPCs harbor a *NAB2-STAT6* fusion, suggesting that meningeal-based HPCs and SFTs are biologically related.

Design: We examined a series of 22 meningeal-based tumors and classified them as SFT, malignant SFT, HPC, or tumors with "intermediate" features using strict morphologic criteria. All tumors were evaluated for CD34 and STAT6 expression by immunohistochemistry and characterized at the molecular level by RT-PCR studies for three common *NAB2-STAT6* fusions (NAB2 exon 4 – STAT6 exon 3, NAB2 exon 6 – STAT6 exon 18 and NAB2 exon 6 – STAT6 exon 17) conducted on paraffin-embedded tissues. Twenty-nine conventional soft tissue-based SFTs were used as a control group.

Results: All meningeal tumors (22/22) showed nuclear expression of STAT6. While SFTs consistently expressed diffuse CD34, the staining pattern in HPCs and intermediate tumors was heterogeneous. *NAB2-STAT6* fusions were identified in 75% (3/4) meningeal SFTs but in only 38% (3/8) cases of meningeal HPC. No cases with intermediate histology (0/8) or malignant SFTs (0/2) harbored these most common fusions. *NAB2-STAT6* fusions were identified in 72% (21/29) soft tissue-based SFTs.

Conclusions: While meningeal-based SFTs and HPCs share STAT6 expression, meningeal HPCs appear to exhibit morphologic differences, variable CD34 expression, and a variable molecular profile, in some cases different from that of most SFTs.

1721 Ablation of b1 Integrin Prevents Locomotor Hyperactivity and Disinhibition-Like Behavior in a Mouse Model of Alzheimer's Disease

Ania Gheyara, Kaitlyn Ho, Weikun Guo, Louis Reichardt, Lennart Mucke. University of California, San Francisco, CA; Gladstone Institute, San Francisco, CA.

Background: Amyloid-β peptides (Aβ) are widely thought to causally contribute to the pathogenesis of Alzheimer's disease. b1 integrin acts as a receptor for Aβ and mediates Aβ-induced neurotoxicity in cell culture models. However, the role of integrin signaling in Aβ-mediated deficits *in vivo* remains uncertain. We wanted to determine whether reduction of b1 integrin can ameliorate behavioral or biochemical abnormalities in human amyloid precursor protein (hAPP) transgenic mice that have pathologically elevated levels of Aβ in the brain.

Design: We bred hAPP mice from line J20 with mice in which the b1 integrin gene was "floxed", and with mice expressing cre recombinase directed by the *Nex* promoter, resulting in mice with or without hAPP that did or did not lack b1 integrin in excitatory forebrain neurons. We then compared the phenotype of the four groups of mice using behavioral, biochemical and pharmacological methods.

Results: b1 integrin ablation prevented locomotor hyperactivity in the open field and disinhibition-like behavior in the elevated plus maze in hAPP mice, but did not ameliorate their learning and memory deficits in the Morris water maze. b1 integrin ablation also did not affect hippocampal levels of soluble Aβ, amyloid plaques, or markers of aberrant neuronal activity such as neuropeptide Y and calbindin. Compared with nontransgenic controls, hAPP mice had increased levels of dopamine receptor 1 (DR1) in the dentate gyrus, which could account for some of their behavioral alterations. In support of this hypothesis, the hyperactivity of hAPP mice was reversed by treatment with a DR1 antagonist, which at the doses used, did not affect the locomotor activity of mice lacking hAPP.

Conclusions: Our findings suggest that the hyperactivity and disinhibition-like behavior of hAPP mice are mediated, at least in part, by b1 integrin in excitatory forebrain neurons. Additional studies are needed to determine the exact relationship between b1 integrin and abnormal dopaminergic function in this hAPP/Aβ-dependent pathogenic cascade. It may also be of interest to further explore the role of b1 integrin in related behavioral abnormalities observed in patients with Alzheimer's disease and in other disorders associated with hyperactivity and disinhibition.

1722 Predictive Value of MGMT Gene Promoter and LINE-1 Methylation Status in Primary Central Nervous System Diffuse Large B-Cell Lymphoma Treated With High-Dose MTX and Radiotherapy

Kanako Hatanaka, Yutaka Hatanaka, Kyoko Fujii, Hiroyuki Kobayashi, Hiromi Kanno, Tomoko Mitsuhashi, Hiroshi Nishihara, Shinya Tanaka, Yoshihiro Matsuno. Hokkaido University Hospital, Sapporo, Japan; Hokkaido University Graduate School of Medicine, Sapporo, Japan.

Background: More than 95% of primary central nervous system lymphomas are diffuse large B-cell lymphoma (PCNS-DLBCL). Although methylation of the O^6-methylguanine-DNA methyltransferase (*MGMT*) gene promoter has been shown to predict a favorable response to temozolomide in patients with PCNS-DLBCL, the predictive impact of tumor DNA methylation in patients who have received standard therapy (high-dose methotrexate plus radiation, HD-MTX+RT) remains unknown. Methylation of long interspersed nuclear element-1 (LINE-1) is known to be a surrogate marker of global DNA methylation.

Design: We analyzed 25 patients (age range 40-77 yr, median 62 yr; M:F=11:14) with histologically proven PCNS-DLBCL, who were treated with HD-MTX+RT at Hokkaido University Hospital and affiliated hospitals during the period 2001-2009. Tumor DNA was extracted from formalin-fixed paraffin-embedded tissues. MGMT expression was assessed by immunohistochemistry (MGMT-IHC), and *MGMT* promoter methylation was analyzed by methylation-specific PCR (MSP). Pyrosequencing was used to determine the methylation status of the CpG island region of LINE-1. We then investigated the correlation of the DNA methylation with overall survival (OS) and progression free survival (PFS).

Results: The MGMT-IHC-negative group (7/25 cases) showed significantly poorer OS than the MGMT-IHC-positive group (p=0.003). Methylation of the *MGMT* promoter (10/22 cases) was significantly correlated with poorer PFS and OS (p=0.029 and p=0.007, respectively). The results of MSP analysis were significantly correlated with those of MGMT-IHC (chi-squared test: p=0.002). A high level of LINE-1 methylation (10/22 cases) was significantly correlated with poor OS (p=0.017).

Conclusions: *MGMT* promoter methylation and high-level methylation of LINE-1 are predictors of poor outcome in patients with PCNS-DLBCL treated with HD-MTX+RT. MGMT-IHC can be used as a routine diagnostic tool for patient stratification.

1723 A Comparative Study of the Intratumor Immune Effect of Dendritic Cell Vaccination and the Conventional Treatment in Glioblastoma

Miguel Idoate, Inigo Arana, Ricardo Diez-Valle, Susana Inoges, Ascension Lopez, Jose Echeveste, Maria Lozano, Sonia Tejada, Francisco Guillen Grima. University Hospital of Navarra, Pamplona, Spain.

Background: A progressive evidence exists that systemic immunotherapy can induce an antitumor response in glioblastomas (GB). Currently, the subcutaneous administration of repeated pulses of mature dendritic cells is considered an especially efficient procedure. There are only a few papers that evaluate the intratumor immune infiltrate in the GB. For this reason, a comprehensive histopathological and clinical study designed to evaluate the effect of vaccines on cellular immune infiltration of GB was carried out.

Design: Sixty complete tumor resection samples from 30 primary GB and their correspondent recurrences of the same number of patients treated by protocolized radio-chemotherapy were studied. From them, 15 patients received subcutaneously injected autologous mature dendritic cells pulses, which were administered until the recurrences. An immunohistochemical study against CD4, CD8, CD16 and NK (Tia-1) cells was obtained. A semiquantitative evaluation of both intensity/activation and the distribution of the infiltrate was carried out by two observers. Several relevant immunological and oncological parameters were studied. A survival statistical evaluation was obtained.

Results: In both groups of GB a rather similar basal immune infiltrate composed by CD8 and CD4 lymphocytes, activated microglia and NK cells of variable intensity and both perivascular and interstitial (homogeneous) patterns was observed. As the basal values were not comparable between both groups, each group was compared with itself. Only in the group of vaccinated GB a significant increase (p=0.05) of the CD8 infiltrate was detected. However, both CD4 infiltrate and microglial activation showed an increase in the vaccinated group, but not in the control group, which was non-significant (p=0.7 and p=0.234, respectively). NK cells showed a non-significant increase (p=0.186) in both groups. In the Cox regression test, the basal activated microglial intensity, but not other immune parameters, correlated with overall survival (HR: 2.20 (IC95%: 1.13-4.31); p=0.02).

Conclusions: The dendritic cell vaccination elicits a specific significant increase in CD8 cells in the GB that is not seen in the control group. In terms of prognostic impact, only the basal activated microglial non-vaccine related correlated with overall survival, which raises an interesting therapeutic approach on this inducible cell.

1724 Gene Expression Differences in Asymptomatic, Middle Aged ApoE4 Homozygotes

Teklu Legesse, Ari Peclovitz, Kimberly White, H Ronald Zielke, Amol Shetty, George Perry, Rudy Castellani. University of maryland Medical Center, Baltimore, MD; Institute for Genome Sciences, Baltimore, MD; University of Maryland, Baltimore, MD; University of Texas, San Antonio, TX.

Background: Attempts at therapeutic intervention in Alzheimer disease (AD) have targeted pathological lesions, most notably amyloid-β (Aβ) plaques. The rationale is based on the amyloid cascade hypothesis, that Aβ is a rate-limiting factor for disease. Attempts at lesion targeting to date, however, have failed. Some research groups have suggested that this requires re-examination of the hypothesis versus earlier intervention.

Design: : We examined the brains of middle aged subjects for Apolipoprotein E (*APOE*) genotype. We selected three homozygous *APOE 4* cases (12X increased risk of AD) and three *APOE2/E3* cases, based on age and RNA integrity. Three brain regions were sampled: Brodmann area 8 which, medial temporal lobe, and cerebellar cortex. The samples were sequenced using the Illumina HiSeq platform and aligned to the reference genome using the splice-aware aligner TopHat. Differential gene expression analysis used the DESeq R package (available from Bioconductor). The read counts were normalized for sequencing depth and distortion caused by high expressed genes. The negative binomial (NB) model was used to test the significance. The differentially expressed genes were deemed significant if the FDR (False Discovery Rate) was less than 0.05, the gene expression was above the 25th percentile and gene showed > 2-fold change difference between the two genotypes. The significant differentially expressed genes were compared across brain region.

Results: Using the strictest parameters, 18 differentially expressed genes were identified. Noteworthy among the 18 genes were major histocompatibility complex loci, and anti-oxidant enzymes, and occurred irrespective of brain region, suggesting a global neuroinflammatory process without regard to lesion vulnerability.

Conclusions: Brains from young individuals with a substantial increased risk for AD (based on APOE genotype) show evidence of on-going neuroinflammation, irrespective

of vulnerability to pathology. These results suggest a global metabolic syndrome, and may constitute the basis for the continued failure of clinical trials. These results further suggest neuroinflammation as a primary target in asymptomatic individuals.

1725 Transcription Factors as Potential Diagnostic Immunostains for Glial Neoplasms

Christopher Liverman, Tarik Tihan, Melike Pekmezci, Mariarita Santi-Vicini, Daniel Martinez, Arie Perry. University of California, San Francisco, CA; Children's Hospital of Philadelphia, Philadelphia, PA.

Background: Immunohistochemistry for glial fibrillary acidic protein (GFAP), the canonical marker for astrocytic neoplasms, is often difficult to interpret. The transcription factor markers SOX2, SOX10 and OLIG2 are increasingly used in the diagnostic workup of brain tumors; however, the staining characteristics of these newer markers are not well defined. Therefore, we analyzed these markers in a variety of primary and metastatic brain tumors.

Design: SOX10, SOX2, OLIG2 and GFAP immunohistochemistry was performed on tissue microarrays (TMA) containing a variety of glial, glioneuronal, non-glial, and metastatic brain tumors. Each case was scored as positive (at least moderate intensity in >10% of cells) or negative for each TMA core. The sensitivity, specificity, positive predictive value and negative predictive value were calculated for SOX2 and OLIG2 as markers of glial neoplasms and for SOX10 as a marker for glial and peripheral nerve sheath tumors.

Results: We analyzed 434 tumors. The immunohistochemical findings for SOX10, SOX2 and OLIG2 are summarized in the Table. SOX10 showed a specificity and positive predictive value of 99% for glial and nerve sheath tumors. OLIG2 was 98% specific for glial neoplasms, with a positive predictive value of 98%. SOX2 was highly sensitive (88%) for glial tumors but had a specificity of only 18%.

	Cases (#)	SOX10 (%Positive)	SOX2 (%Positive)	OLIG2 (%Positive)
ATRT	17	0	59	6
Medulloblastoma	42	0	95	0
Meningioma	16	0	80	0
Craniopharyngioma	20	0	84	0
SEGA	5	0	100	0
Ganglioglioma	23	39	96	33
Central Neurocytoma	3	0	100	0
DNET	11	100	90	75
Ependymoma	27	7	93	0
Pilocytic astrocytoma	34	76	78	54
Astrocytoma, grade II and III	32	63	85	65
GBM	61	44	86	44
Oligodendroglioma	38	50	97	90
Cellular schwannoma	12	100	92	
MPNST	40	25	78	
Metastatic adenocarcinoma	22	0	75	5
Metastatic non-adenocarcinoma	16	0	60	6

Conclusions: OLIG2 is a useful marker for astrocytic and oligodendroglial tumors with a high specificity and positive predictive value. SOX10, a sensitive marker for low grade peripheral nerve sheath tumors, is potentially useful as a specific marker for glial tumors. SOX2, while highly sensitive, is too non-specific to be useful in the workup of glial neoplasms.

1726 Targeted Next Generation Sequencing and Methylguanine-DNA Methyltransferase Methylation in Glioma Patients

Ekrem Maloku, Jason Peterson, Emmeline Liu, Christopher Amos, William Hickey, Lara Ronan, Camilo Fadul, Gregory Tsongalis, Francine de Abreu. Dartmouth-Hitchcock Medical Center, Lebanon, NH; Geisel School of Medicine, Hanover, NH.

Background: Glioblastoma represents the most common primary intrinsic malignant brain tumor diagnosed each year in the United States. It is known that the DNA repair enzyme O^6-methylguanine-DNA methyltransferase (MGMT) antagonizes the genotoxic effects of alkylating agents. Many studies emphasize MGMT promoter methylation as the key mechanism of MGMT gene silencing, predicting a favorable outcome in patients with glioblastoma who are exposed to alkylating agent chemotherapy. Here we present data from a targeted next generation sequencing assay in conjunction with MGMT promoter methylation status in a cohort of glioblastoma patients.

Design: Genomic DNA was extracted from 27 FFPE glioblastoma samples. Ten nanograms of DNA were used to create barcoded libraries which were multiplexed on Ion Torrent 318v2 chips and sequenced using the AmpliSeq Cancer Hotspot Panel v2. Variants were identified using the Ion Torrent Variant Caller Plugin (v4.0.2). Variant annotation and functional predictions were performed using Golden Helix SVS (v.7.7.8). For MGMT methylation analysis, 50 ng of DNA were bisulfite converted using MethylEdge™ Bisulfite Conversion System and MGMT methylation status was determined using the MethyLight.

Results: Of the 27 cases analyzed 29.6% were wild type and 70.4% were positive for hotspots tested in the panel. Clinically actionable variants were identified in IDH1 (18.5%), PIK3CA (3.7%), CDKN2A (7.4%), and MET (7.4%). Currently non-clinically actionable variants were identified in TP53 (37.0%), PTEN (11.1%), and EGFR (3.7%). In the 5 samples where MGMT promoter methylation was identified, variants were identified in the IDH1, EGFR, and TP53 genes. Among the samples negative for MGMT methylation status, three had a common mutation in IDH1 gene.

Conclusions: Somatic mutation is common in glioblastoma giving rise to numerous clinically actionable variants associated with response to therapy. Similarly, MGMT promoter methylation can predict a favorable outcome in patients who are treated with alkylating agent chemotherapy such as temozolomide. Routine testing for these molecular markers is imperative for the success of a personalized therapeutic management strategy.

1727 PDL-1 Expression Differs Between Glioblastoma Subtypes

Maria Martinez-Lage, Timothy Lynch, Sharmistha Pal, Yingtao Bi, Ramana Davuluri, Laura Roccograndi, Robert Bailey, Arati Desai, Donald O'Rourke, Nadia Dahmane. University of Pennsylvania, Philadelphia, PA; William Penn Charter School, Philadelphia, PA; Northwestern University, Chicago, IL.

Background: Glioblastoma (GBM) is the most common primary brain tumor, with an average survival of 15-18 months. Four subtypes have been identified by RNA profiling. Recently, immunotherapy has emerged as a promising adjuvant approach. PDL-1 is a protein involved in T-cell inhibition which can be expressed in tumor cells. We analyzed expression of PDL-1 in GBMs by immunohistochemistry (IHC), and evaluated association with molecular subtype.

Design: IHC for PDL-1 (clone E1J2J, Cell Signaling, 1:4500) was performed in a tissue microarray of GBM obtained from the Brain Tumor Tissue Bank. The samples included 18 neural (N), 15 proneural (PN), 12 mesenchymal (M) and 11 classical (C) GBM, as per RNA expression profile. Each tumor was sampled at least in triplicate, with tumors showing higher morphologic heterogeneity sampled up to 6 times. PDL-1 expression was evaluated for each core and averaged across each case using the H-score, a summation of the percentage of cells stained at each intensity level multiplied by the weighted intensity as strong (3), moderate (2), weak (1) or blush (0.5). Statistical analysis was performed using GraphPad InStat software.

Results: 56 patients (52% male) were included, with average age of 60 (range 39-77), and median survival 12 months (range 0->120). Median survival by group was 11 (PN), 15.5 (N), 13 (C) and 9.5 (M). PDL-1 expression was seen at least focally in all but one case (98%), in the cytoplasm and membranes of tumor cells (Figure 1). Median H-score overall was 50.02, with a range of 0-280 and SD 47.02. By group, median H-score was 20 (PN), 47.5 (N), 75 (M) and 20 (C). These were significantly different across groups by ANOVA (p 0.0217), with the highest difference existing between the PN and the M groups. There were no significant differences in survival across groups and no correlation between PDL-1 expression and survival.

Conclusions: PDL-1 can be detected at least focally in a majority of GBM, and it is differentially expressed amongst molecular subtypes, with higher expression seen in mesenchymal subtype and lowest in proneural and classical subtypes. This finding may offer biological support to the use of PDL-1 inhibitors in the treatment of certain GBM cases.

Figure 1. PDL-1 staining patterns in GBM and semiquantitative H-scores. 100x. A: Mesenchymal subtype with moderate to strong diffuse membranous staining, score 250 (3x50% + 2x50% + 1x0%). B: Classical subtype with scattered strong cytoplasmic staining, score 110 (3x20% + 2x10% + 1x20%).C. Proneural subtype with scattered granular cytoplasmic staining, score of 50 (3x0% + 2x20% + 1x10%). D: Neural subtype with diffuse weak membranous staining, score of 85 (3x0% + 2x5% + 1x75%).

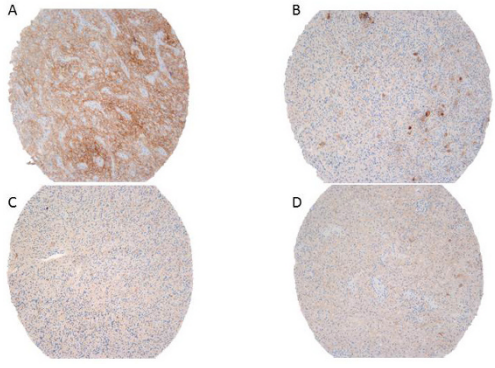

1728 Cell Signalling Factors in Pilocytic Astrocytomas: p4E-BP1 and pMAPK as New Therapeutic Targets

Elena Martinez-Saez, Jessica Camacho, Vicente Peg, Teresa Moline, Javier Hernandez-Losa, Joan Carles Ferreres-Pinas, Santiago Ramon y Cajal. Vall d'Hebron University Hospital, Barcelona, Spain.

Background: EGFR and cell signalling factors play an important role in gliomas. 4E-binding protein-1 (4E-BP1) factor, eIF4E and their phosphorilated forms (p4E-BP1 and peIF4E) control the expression of genes involved in cell cycle and cell proliferation (cyclin D1, myc, VEGF, FGF, survivin). p4E-BP1 and eIF4E have been shown to be a prognostic factor in malignant astrocytomas and no data has been reported concerning pilocytic astrocytomas (PAs). PAs are mostly grade I tumours, located in posterior fossa and affecting children or young patients. Alterations in the BRAF gene (KIAA-BRAF

fusions, BRAF V600E mutation) are the most consistent molecular changes found so far. In this study we evaluated the expression of cell signalling factors in PAs and compare them to diffuse astrocytomas.
Design: Twenty-one PAs and 104 diffuse astrocytomas have been collected from the Vall d'Hebron University Hospital files (20 grade II astrocytomas, 24 anaplastic astrocytomas and 60 glioblastomas (GBMs)). Immunohistochemical stains for EGFRvIII, pMAPK, 4E-BP1, p4E-BP1, eIF4E, peIF4E, cyclin D1 and Ki67 were performed in all tumours; p16 only in PAs. Protein expression levels were semiquantitatively evaluated as percentage and intensity of stained cells (histo-score), and percentage of staining for p16, Ki67 and cyclin D1.
Results: PAs and GBMs showed similar levels of 4E-BP1 and p4E-BP1, whereas eIF4E and peIF4E were significantly higher in GBMs. Interestingly, levels of cyclin D1 and pMAPK in PAs surpassed those in GBMs. Diffuse astrocytomas showed a progressive increase in EGFRvIII, 4E-BP1, p4E-BP1, eIF4E, peIF4E and cyclin D1 expression according to the grade. PAs showed low proliferative activity and high p16 expression.
Conclusions: Surprinsingly, PAs display similar or higher levels of some of the cell-signalling factors involved compared to GBMs. The signalling cascade seems to be intercepted at eIF4E level. These results support the use of inhibitors of 4E-BP1 and MAPK phosphorilation in PAs and open new avenues in the understading of the biology of PAs. Furthermore, the overexpression of p16 together with the low proliferative activity highlights the oncogenic-induced senescence phenomenon in PAs.

1729 Orphan G Protein Coupled Receptors (GPCRs) as Molecular Markers for Glial Cell Tumors

Nitin Marwaha, Grant Kolar, Gina Yosten. Saint Louis University School of Medicine, St. Louis, MO.
Background: It is becoming increasingly clear that the morphological patterns that describe the classical definitions of various brain tumors represent categories of disease. In the case of glioblastoma a striking stratification based upon microarray profiles recently revealed separate but specific pathways of gene activation leading to a similar morphological phenotype. Various morphological phenotypes of glioblstoma likely represent variations in gene expression within neoplastic astrocytes. GBM is the most common brain tumor in adults. It is noted however that variability in the course and prognosis of GBM exists with some individuals surviving as much as 5 years after diagnosis. Recently the stratification of primary and secondary GBMs based on IDH1 raises the possibility that more than one pathway leads to the morphologically based disease. Other potential markers may help us to stratify GBMs into different treatment groups and as a consequence prognostic categories. GPCRs represent the largest target group of pharmaceutical therapeutics. Approximately 130 GPCRs however remain orphan receptors without known ligands. These are often excluded in genome wide expression studies. We hypothesized that within this group several receptors would be expressed in GBMs well above that seen in the surrounding brain presenting potential targets for therapy, earlier diagnostics, or post-therapeutic surveillance.
Design: RNA was collected from GBM samples and normal brain tissue from similar brain regions. Using a unique multiplex PCR-based MasterMix technology, samples were screened for the expression of all known orphan GPCRs. Bioinformatic and Pathway analyses were applied to determine clustering of GBM subtypes. Orphan GPCRs with high association to GBM were further evaluated in GBM tissue samples using immunohistochemistry.
Results: Based on orphan GPCR expression compared to normal tissue, we were able to categorize GBMs into molecular subtypes, particularly with respect to orphan GPCRs bearing homology to angiogenesis-related receptors (e.g., GPR146 and GPR56). Immunohistochemistry analyses of GBM-associated orphan GPCRs revealed unique patterns of expression of these GPCRs within GBM samples, some of which was confined specifically to the tumor vasculature.
Conclusions: From these data we conclude that orphan GPCRs may potentially serve as diagnostic markers with possible prognostic consequences. In addition, orphan GPCRs may represent novel therapeutic targets for the treatment of this deadly brain tumor.

1730 Genomic Profile of Chordoid Meningiomas

David Meredith, Malak Abedalthagafi, Wenya Linda Bi, Ian Dunn, Azra Ligon, Brian Alexander, Sandro Santagata. Brigham & Women's Hospital and Harvard Medical School, Boston, MA.
Background: Chordoid meningioma is a rare variant of the WHO grade II atypical meningioma with a propensity for aggressive behavior and increased likelihood of recurrence. It's characterized by strands and cords of meningothelial cells arranged in a myxoid or mucinous background. We present here the genomic signatures of seven cases of chordoid meningioma.
Design: We used genomic techniques to characterize the copy number alterations and DNA aberrations in seven chordoid meningioma from five females and two males. The mean age of the patients at diagnosis was 51 years. Four cases were skull based and three were in the convexity. Median follow up was 61 months. Two patients had recurrent tumor; three patients had received radiation. Array - based comparative genomic hybridization (aCGH Oncoopy) was performed on 7 samples and targeted next generation exonic sequencing for 562 genes (Oncopanel) was performed on 5 unmatched samples to identify tumor - specific genomic changes in FFPE clinical samples.
Results: Loss of 1p was the most frequent copy-number (CNVs) alteration, occurring in 6/7 cases. Frequently observed alterations included: Monosomy 22 (4/7), Monosomy 14 (3/7), 6q (2/6), 7p (1/7), 10q and 18q was not observed in any case. Loss of CDKN2A 9p21 was seen in 1 case suggesting anaplastic transformation. Exonic sequencing did not show mutations in some of the genes that are commonly altered in more common types of meningioma including – : SMO, AKT, TRAF7, and KLF4 – but in frame deletions were found in NF2 in two of the cases. Other mutations, which need further validation, were observed in chromatin remodeling genes ARID1A, MLL3, and KDM6A as well as important signaling molecules NOTCH2, FGFR3 and ERBB3, ROS1 and NFKBIA.
Conclusions: Chordoid meningiomas show many of the Oncocopy CNVs that are found in more traditional WHO grade II and III meningioma. Genetic aberrations in NF2 and genes involved in chromatin remodeling and other signaling pathways may contribute to the pathogenesis of chordoid meningioma.

1731 Evaluation of Hypermetabolic Neurons in Seizure Onset Zones of Children With Focal Cortical Dysplasia

Lili Miles, Hansel Greiner, Francesco Mangano, Paul Horn, Michael V Miles. Cincinnati Children's Hospital, Cincinnati, OH.
Background: Focal cortical dysplasia (FCD) is a common cause of intractable epilepsy in children. Scattered hypermetabolic neurons (HMN), easily identified by their intense reactivity to cytochrome *c* oxidase (COX) immunohistochemical (IHC) stain, have been reported in the seizure onset zone (SOZ). Recently, COX biochemical deficit was found in PET hypometabolic regions of pediatric patients with FCD Type II (FCDII) vs FCD Type I (FCDI), but without control comparison (*Epilepsia* 2014;55:1415-22). We propose to evaluate COX^+ HMN in patients with FCD subtypes vs controls, and to determine if differences in COX IHC counts are associated with COX biochemical differences in SOZ.
Design: This retrospective review evaluated patients having surgery for intractable epilepsy (2010-11). Inclusion criteria: age 6mo-18y; diagnosis of FCDI or FCDII; biochemical analysis of COX activity in SOZ cortex. Autopsy specimens were collected for IHC controls. SOZ specimens were identified by intracranial EEG during surgery. Neuropathologic methods were published previously (*JNEN* 2013;72:884-91). After screening the entire section of SOZ tissue, COX^+ HMN were counted in 4 representative high-power fields (hpf), and averaged. COX and citrate synthase (CS) activities in SOZ were measured spectrophotometrically.
Results: 22 patients (7 FCDI/15 FCDII) met the inclusion criteria. 5 autopsy cortex specimens were controls. Although COX^+ HMN counts were significantly increased in both FCD types vs controls, they were also less in FCDII vs FCDI. COX biochemical activity was decreased in the FCDII vs FCDI. CS activity, a marker of mitochondrial mass, was similar in FCD groups.

	FCDI (n=7)	FCDII (n=15)	Controls (n=5)
Total COX+ HMN/hpf	43±6#	24±16*	19±7+
COX biochemical activity ([/min]k-1/mg prot)	2.7±0.3	2.2±0.6*	not done
CS activity (µmol/min/mg prot)	0.25±0.09	0.25±0.07	not done
P#vs controls; *vs FCDI; +vs 3 gps. Mean±SD.			

Conclusions: This is the first study to demonstrate that COX^+ HMN counts are increased in FCD SOZ, FCDI>FCDII>controls. These results suggest that increased COX^+ HMN in FCD are linked to uncontrolled seizures. Trends for COX^+HMN count and COX activity are similar between FCDI and FCDII. Although further study is needed, COX^+ HMN count may be a novel biomarker of COX activity in mitochondria of FCD patients.

1732 Neuropathology of Fatal Head Trauma in Children Under 3 Years Old

Douglas Miller, Shunhua Guo, Emily Coberly, Carl Stacy. University of Missouri School of Medicine, Columbia, MO.
Background: Debate continues over the specificity of pathological findings in pediatric head trauma. It is claimed that subdural hematomas (SDH) and retinal hemorrhages (RH) can result from raised intracranial pressure of any cause.
Design: We reviewed autopsy findings for all child deaths under age 3 done by our Medical Examiner from 1/1/2008 through 12/31/2013. All had full autopsies, including brain examination by a neuropathologist. In about half the cases either the eyes were examined or the posterior globes were removed to examine retinas histologically and in over 1/3 of cases the spinal cords were also examined.
Results: From about 3400 autopsies we had 105 deaths of children under age 3. From police investigations, autopsy findings, and subsequent legal findings 15 deaths were attributed to fatal head trauma. Two trauma deaths were documented vehicular accidents; the other 13 were determined to be inflicted trauma. Significant body injuries were present in 8/13, 11 had externally evident blunt head trauma, 4 had skull fractures, 8 had significant SDH, 1 had a small focal SDH with older subdural membranes, 9 had subarachnoid hemorrhages, 2 had cerebral contusions, and 6 had deep brain hemorrhages. All of the trauma victims had swollen heavy brains, 11 had 1 or more herniations, 8/13 had some focal hypoxic/ischemic neuronal injury, and 3 had diffuse axonal injury. RH was diffuse and bilateral in 5 and focal or unilateral in 2; 5 also had optic nerve sheath hemorrhage. Only 1/13 had hemorrhage, in the cervical spinal roots and cord parenchyma. Both accident victims had external head injuries, skull fractures, SDH, and deep brain hemorrhages; 1 had cerebral contusions. One each had cerebral and spinal subarachnoid hemorrhage, and 1 had RH without optic nerve sheath hemorrhage. Of the 90 non-trauma deaths, including cases of SIDS, meningitis/encephalitis, sepsis, pneumonia, congenital heart disease, Leigh's Disease, and severe prematurity, none had SDH (4 had older membranes), 2 had focal small subarachnoid hemorrhages, 36 had neuronal hypoxic/ischemic changes, and 8 had cerebral edema (6 with herniations). Eyes or retinas in 44 of these showed no RH, one optic nerve sheath hemorrhage. Twenty-three examined spinal cords were unremarkable.
Conclusions: Acute SDH, deep brain hemorrhage, and RH (particularly when diffuse and bilateral), especially in combination, are diagnostic of severe head trauma and is most often from inflicted trauma.

1733 MAPK Activation and HRAS Mutations Identified in Pituitary Spindle Cell Oncocytoma

Michael Miller, Wenya Linda Bi, Lori Ramkissoon, Malak Abedalthagafi, Yun Jee Kang, David Knoff, Ian Dunn, Patrick Wen, David Reardon, Brian Alexander, Edward Laws, Jr., Rameen Beroukhim, Keith Ligon, Shakti Ramkissoon. Brigham & Women's Hospital, Boston, MA; Dana-Farber Cancer Institute, Boston, MA.

Background: Pituitary spindle cell oncocytoma (SCO) is an uncommon pituitary neoplasm that presents with mass effect on adjacent neurovascular structures, similar to non-hormone-producing pituitary adenomas. Spindle cell oncocytomas are thought to derive from native folliculostellate cells; however, little is known about their molecular etiology.

Design: Whole exome sequencing (WES) was performed on four SCO cases (with matched normal control) to assess somatic mutations and copy number alterations. Additionally, we performed immunohistochemistry to evaluate MAPK and PI3K signaling pathway activation in these tumors.

Results: Analysis of the initial WES dataset revealed a low mutation rate and a copy-neutral profile, which is consistent with the low-grade nature of this tumor. However, we identified a co-occurring somatic *HRAS* (p.Q61R) activating point mutation and a *MEN1* frameshift mutation (p.L117fs) in one SCO. WES data analysis for the other 3 samples is in progress. Immunohistochemistry across the SCO cohort demonstrated robust MAPK activity in all cases (n=4) as evidenced by strong p-ERK staining, while the PI3K pathway did not exhibit activation based on low p-AKT levels.

Conclusions: We identified the MAPK signaling pathway as a novel therapeutic target for spindle cell oncocytoma. In all four cases we found protein evidence that the MAPK pathway is activated in these tumors and may contribute to cell proliferation. Sequencing analysis revealed *HRAS* and *MEN1* mutations in the first SCO analyzed by WES. As complete surgical resection is not always possible for these tumors, targeted molecular therapies may inhibit more aggressive tumors.

1734 A Precursor Lesion To AT/RT? A Case of AT/RT in Association With a Lower Grade SMARCB1-Deficient Neoplasm

Stewart Neill, Krishanthan Vigneswaran, Chad Holder, Debra Saxe, Michael Rossi, Matthew Schniederjan. Emory University, Atlanta, GA.

Background: Atypical teratoid/rhabdoid tumors (AT/RTs) are WHO Grade IV embryonal neoplasms of the central nervous system (CNS) that may display a wide variety of histologic appearances. Typically these tumors show "rhabdoid" cells with prominent nucleoli and eosinophilic cytoplasmic inclusions. Uniting these tumors is the finding of alterations in *SMARCB1* (*INI1*) on 22q11.23 leading to loss of protein expression, placing these tumors within the family of malignant rhabdoid tumors. AT/RTs tend to arise *de novo*; no definite precursor lesion has been identified. We describe an AT/RT associated with an SMARCB1-deficient tumor that appeared lower grade by histologic, immunohistochemical (IHC), and copy number (SNP-CN) analysis.

Design: A 32 year-old female presented with complaints of headache, lethargy, and altered mental status of 2 weeks duration. Her history was significant for resection of a foramen magnum schwannoma in 2007 with post-operative MRI that demonstrated increased T2 signal centered within the left cingulate gyrus. Biopsy of this lesion in 2009 proved non-diagnostic. The patient was lost to follow up until she presented to the emergency room where an MRI was obtained that demonstrated a 5 cm intra-axial enhancing lesion centered in the left frontal lobe; the lesion was urgently resected.

Results: Permanent sections showed dense rhabdoid tumor cells with abundant necrosis. The adjacent brain was infiltrated by small, banal glial-appearing cells; involved neurons showed granulovacuolar degeneration and neurofibrillary tangles. The embryonal proliferation and the banal infiltrate were both negative for SMARCB1 protein by IHC. The embryonal cells showed brisk reactivity for MIB-1 IHC; the banal infiltrate displayed minimal reactivity. Affymetrix Oncoscan SNP-CN arrays performed separately on both tumor components showed that the embryonal cells had homozygous deletion of the *SMARCB1* locus as well as trisomy 8 and a focal loss on 13q. The lower-grade appearing component had loss of *SMARCB1* as the only detected copy number abnormality.

Conclusions: AT/RTs are embryonal neoplasms of the CNS within the family of malignant rhabdoid tumors. Though these tumors have been rarely described to arise within lower-grade lesions, a definite precursor lesion has yet to be identified. We demonstrate an AT/RT arising in association with an SMARCB1-deficient neoplasm that is lower grade by histologic, immunohistochemical, and SNP-CN analysis.

1735 Radiology Misleading Pathology

Larry Nichols, Ashley Porter, Charles Handorf. University of Tennessee College of Medicine, Memphis, TN.

Background: A case of an actinomycotic brain abscess with a radiologic misdiagnosis of high grade glioma leading to a brain biopsy pathologic misdiagnosis with fatal results (23 years ago at another institution) used for medical education prompted a question how often this happens and a search of the medical literature revealing a dearth of data.

Design: All brain biopsy diagnoses over a recent 2-year period were compared with the radiologic diagnoses that prompted the biopsies. Both the radiologic and pathologic diagnoses were categorized as low grade glioma, high grade glioma, other brain primary tumor, lymphoma, metastasis, meningioma, hemorrhage, infection or other. Assuming the pathologic diagnosis was correct, the corresponding radiologic diagnoses were categorized as helpful, misleading or neutral.

Results: There were 208 brain biopsies, 8 signed out as low grade glioma, 49 high grade glioma, 18 other brain primary tumor, 6 lymphoma, 50 metastasis, 40 meningioma, 9 hemorrhage, 3 infection and 25 other diagnoses or no diagnosis. Of 208 radiologic diagnoses, we classified 133 (64%) as helpful, 29 (14%) as misleading and 46 (22%) as neutral. In all 3 cases of brain biopsies signed out as infection, the radiologic diagnosis was misleading. In a case of toxoplasmosis, the radiologic diagnosis was cerebrovascular accident versus brain mass. In one case of brain abscess, the radiologic diagnosis was high grade glioma versus metastasis. In another case of brain abscess, the radiologic diagnosis was glial tumor.

Conclusions: Neuroradiologic diagnoses are usually helpful to pathologists signing out brain biopsies. The fact that all 3 brain infections diagnosed by biopsy in our study had a preceding radiologic diagnosis of tumor or a differential diagnosis not including infection suggests that the relative rarity of these conditions compared to tumors and the similarity of the radiologic findings to those of tumors make it difficult for radiologists to accurately differentiate them from tumors, that brain biopsies are important for differentiating them and that pathologists must be aware of the likelihood that the radiologic diagnosis will be misleading in cases of brain infection.

1736 Expression of SERPING1 Is Increased in Reactive Astrogliosis Associated With Neuroinflammation

Amber Nolan, Nicole Croom, Han Lee, Marta Margeta. University of California, San Francisco, CA.

Background: Reactive astrogliosis was once thought of as a stereo-typed response to injury. However, recent gene expression profiling data suggests that astrocytic reaction is heterogeneous, with gene expression patterns that depend on the original insult and thus provide candidates for new reactive astrocyte markers that will be clinically useful in differentiation of equivocal pathologic states. SERPING1 (also known as C1 inhibitor), a serine protease inhibitor which primarily functions to inhibit the complement system, was recently shown to be preferentially expressed in a mouse model of inflammatory brain injury compared to brain ischemia. To asses if this association holds true in human disease, we analyzed expression of SERPING1 using immunohistochemistry on paraffin-embedded tissue from surgical and autopsy cases of encephalitis, cerebral ischemic infarct, and pathologically unremarkable brain tissue. We also explored the pattern of SERPING1 expression in astrocytic tumor cells from glioblastoma (WHO grade IV) cases.

Design: We identified 8 encephalitis/meningioencephalitis cases, 7 ischemic infarcts (both subacute and chronic stages), 8 glioblastomas (WHO grade IV), and 10 controls from both surgical and autopsy cases. Immunohistochemistry for GFAP and SERPING1 was performed. For SERPING1, the intensity of cytoplasmic staining was semi-quantified using a 4-tiered scale (0-3). As a separate parameter, we also quantified the fraction of astrocytes demonstrating both GFAP and SERPING1 staining.

Results: Human pathology replicates mouse model data, demonstrating higher levels of SERPING1 expression in astrocytes and endothelial cells in encephalitis cases compared to ischemic infarcts ($p<0.05$). In addition, a higher fraction of SERPING1+/GFAP+ cells were present in inflammatory compared to ischemic cases ($p<0.01$). Neoplastic glial cells in glioblastoma cases stain with SERPING1, although at lower levels compared to GFAP, and with an angiocentric pattern. Control brain tissue shows only minimal SERPING1 staining in pyramidal neurons, few astrocytes, and rare endothelial cells.

Conclusions: These results confirm that SERPING1 expression is upregulated in inflammatory compared to ischemic astrogliosis and suggest that SERPING1 may be a clinically useful marker of neuroinflammation in biopsies with otherwise non-diagnostic material. Given the recently established role of complement in the synapse pruning, increased expression of SERPING1 by neurons and reactive astrocytes in neuroinflammatory conditions may be important for limiting the excessive synapse loss.

1737 High Percentage of IDH1 (R132H) False Negative Cases in Post-Surgical Low-Grade Glioma Specimens With Significant Cautery Artifact By Immunohistochemistry

Jorge Novo, Brett Mahon, Leonidas Arvanitis. Rush University Medical Center, Chicago, IL.

Background: Differentiation of infiltrating malignant glial cells and reactive gliosis is very challenging in small post-surgical specimens. IDH1 (R132H mutant) immunostain is a great tool that can identify single infiltrating tumor cells with a very high sensitivity and specificity. We evaluated the pattern of immunoreactivity of IDH1 (R132H) antibody in small-post surgical specimens with varying degrees of cautery artifact.

Design: Since the implementation of IDH1 (R132H mutant) immunostain in our laboratory (February 2013), we retrieved 31 cases of infiltrating low-grade gliomas (24 diffuse astrocytomas and 7 oligodendrogliomas). From these 31 cases, we identified 8 cases that were re-excisions for evaluation of tumor recurrence. All these post-surgical specimens contained equivocal infiltrating tumor cells among marked reactive changes. We evaluated the pattern of IDH1 immunoreactivity and correlated the results with molecular studies.

Results: IDH1 immunostain revealed positive immunoreactive cells in 4/8 (50%) post-surgical samples, whereas in 4/8 (50%), IDH1 was completely negative. With high probability of tumor still present, molecular studies were done, and were subsequently positive for IDH1 (R132H) mutation in all of the 4 negative cases. The 4 negative cases showed various amounts of cautery artifact (at least 20%), whereas the 4 positive cases showed minimal to none. In 2 of the 4 positive cases, there was focal loss of IDH-1 immunoreactivity near areas of minimal cautery.

Conclusions: We identified 4 cases of post-surgical specimens with significant cautery artifact that were falsely negative for IDH-1, which were confirmed mutation-positive later by molecular studies. Caution is needed when interpreting negative IDH1 immunoreactivity in post-surgical samples with cautery, since the antibody appears to be very sensitive to this artifact. Further studies resistant to cautery artifact can be performed for definite identification of infiltrating tumor cells.

1738 Correlation of Maspin Expression and Vasculogenic Mimicry in Uveal Melanoma

Lais Osmani, Brian Werstein, Andre Kajdacsy-Balla, Jose Cursino, Amy Lin. University of Illinois, Chicago, IL; Clinica de Olhos Cursino, Taubate, Sao Paulo, Brazil.

Background: Maspin is a serine protease inhibitor that has been shown to inhibit tumor growth and metastasis in multiple cancers. Depending on the tumor type, maspin can localize to the nucleus, cytoplasm, cell surface or extracellular space. Maspin's sub-cellular localization as well as its tissue context may account for the differences in prognostic implications that maspin expression has in different tissues. Uveal melanoma is the most prevalent primary intraocular cancer affecting adults. In uveal melanoma, the formation of looping vasculogenic mimicry (VM) channels is strongly associated with death from metastatic melanoma. Recent studies have found a negative correlation between maspin expression and the occurrence of VM in non-small cell lung cancer. Other studies suggest maspin's possible involvement in the inhibition of the development of VM channels. The aim of this study was to correlate maspin expression with the presence of VM in uveal melanoma.

Design: A tissue microarray, comprised of cores taken from uveal melanoma specimens derived from 92 patients, was stained with an anti-maspin antibody. Each core was previously characterized for cell type (i.e., spindle, epithelioid, and mixed) and for the presence of looping VM patterns. Localization of maspin immunoreactivity (i.e. nucleus, cytoplasm, or membrane) was noted for each core. Staining intensity and the proportion of cells in a core that stained for maspin were used to create a histochemical score for each core. The relationships between maspin expression and looping VM patterns, as well as between maspin expression and cell type (epithelioid, spindle and mixed) were determined using statistical analyses.

Results: Maspin expression was localized to the cytoplasm in all specimens. There was no statistically significant correlation between maspin expression and the presence of VM, or between maspin expression and cell type.

Conclusions: Unlike the negative correlation between maspin expression and VM in non-small cell lung cancer, there was no statistically significant correlation between maspin expression and VM in uveal melanoma. This suggests that maspin may play a role in VM in some types of tumors while not playing a role in others. Cytoplasmic subcellular localization in our study adds to the complexity of the different functions of maspin depending on subcellular localization and tissue context.

1739 Diagnostic Utility of IDH1, ATRX Immunohistochemical Markers and 1p/19q Status for Intermediate Grade Diffuse Gliomas

Buge Oz, Nil Comunoglu, Neslihan Kaya, Onur Dulger, Sebnem Batur. IU Cerrahpasa Medical Faculty, Istanbul, Turkey.

Background: Gliomas, the most common primary brain tumors, are histopathologically classified primarily into prognostically distinct diffuse astrocytomas or oligodendrogliomas. However, with the exception of 1p19q codeletion in oligodendrogliomas, no other markers reliably differentiate these gliomas. We herein this study tried to reclassify intermediate grade diffuse glioma cases, histopathologically diagnosed on H-E stained slides, with the aid of immunohistochemical markers IDH-1, ATRX and 1p19q deletion status. We aimed to designate diagnostic significance of status of immunohistochemical markers IDH-1, ATRX and deletion of 1p19q.

Design: In first step fourty five archival cases were diagnosed with only H&E stained slides. In second step, all cases were immunostained for IDH1, ATR-X, 1p/19q status was assessed by means of FISH. All cases were re-classified with immunohistochemical and FISH results.

Results: Among 45 glioma cases 9 cases classified as oligodendroglioma (OD), 2 cases as anaplastic oligodendroglioma (AOD), 15 cases as oligodendroglial component predominant oligoastrocytoma (O-AO), 8 cases as astrocytic component predominant oligoastrocytoma (A-AO), 8 cases as mixed OA (MOA), 1 case as anaplastic oligoastrocytoma (AOA),1 case as anaplastic astrocytoma (AA), 1 case as astrocytoma. IDH1 immunopositivity was detected in 66 % of OD, 100% (2 cases) of AOD , 80% of O-OA, 87% of A-OA , 87 %of MOA , 100% (1 case) of AOA , 100% (1 case) of astrocytoma. One AA case was immunogative with IDH-1. Loss of ATR-X expression wasn't detected in 66 % of OD, 100% (2 cases) of AOD , in 33% of O-OA, in 25% of A-OA , in %25 of MOA. In 1 AA case and 1 astrocytoma case, loss of ATRX expression were detected. 1p/19q co-deletion was detected in 100 % of OD, AOD, AOA, in 46% of O-OA, in 37% of A-OA , in 62% of MOA. 14 cases were re-classified depending on these results.

Conclusions: Our results showed ATRX status helps to re-classify oligoastrocytomas, since ATRX loss is a hallmark of astrocytic tumors.Loss of heterozygosity of chromosomes 1p and 19q (LOH 1p19q) is the genetic hallmark of oligodendroglial differentiantion.

1740 Pathologic Features of Silent Intralesional Microhemorrhage in Arteriovenous Malformations

Melike Pekmezci, Jeffrey Nelson, Helen Kim, Christopher Hess, Michael Lawton, Tarik Tihan. University of California, San Francisco, CA.

Background: Brain arteriovenous malformations (bAVMs) present significant morbidity and mortality due to intracranial hemorrhage (ICH). We have previously shown that "silent intralesional microhemorrhage" (SIM) is a biomarker for the risk of ICH. New methods to detect SIM present an opportunity to improve risk stratification. In this study, we have evaluated the clinical and morphological characteristics of bAVM to establish a pathological assessment strategy.

Design: We have identified bAVMs diagnosed at UCSF between 1990 and 2011. Patients who were included in our discovery cohort and patients with incomplete clinical or pathology data were excluded. Histological descriptors were classified using a 5-point scale (0=absent, 1 through 4=number of quartiles involved). Statistical analyses used Intercooled Stata V12 and $P<0.05$ was accepted as significant.

Results: Among 555 patients identified through a database search, 251 patients fulfilled the inclusion criteria. There were 125 females and 126 males with a mean age of 34.2 $\pm$ 13 years. Presence of histological features in the group was as follows: hemosiderin in 48%, macrophage infiltrate in 57%, calcification in 13%, dense fibrosis in 98%, extravasated erythrocytes in 42%, fibrin thrombi in 9%, lymphocyte infiltrate in 41%, and smooth muscle proliferation in 95%. ICH, either at the time of initial diagnosis or follow-up, was associated with presence of hemosiderin, deep location and exclusively deep venous drainage, and first two remained significant in multivariate analyses ($p<0.026$). AVMs with hemosiderin (n=120) were more likely to present with ICH (58%) than AVMs without hemosiderin (n=131, 37%, $p<0.001$). Amount of hemosiderin showed significant correlation with the amount of macrophages, lymphocytic infiltrate and dense fibrosis ($p<0.001$ for all).

Conclusions: Initial presentation with ICH is more common among bAVMs with hemosiderin, validating the role of SIM for the risk stratification. For this finding to be useful in patient management, it is essential to develop novel tools which may identify SIM on imaging. Future studies with radiology-pathology collaboration aiming towards identification of hemosiderin, lymphocytes and macrophages in bAVMs in vivo may provide the means to detect SIM.

1741 Telomere Maintenance Mechanisms in Ependymal Tumors

Melike Pekmezci, Tarik Tihan, Roxanne Marshall, Arie Perry, Kyle Walsh. University of California, San Francisco, CA.

Background: Telomere maintenance is essential for the continuous proliferation of neoplastic cells. Activating mutations in the promoter of *Telomerase Reverse Transcriptase* (*TERT*) have been observed in several tumor types. Alternatively, telomere maintenance can be achieved by mutations in the *ATRX* gene (alpha thalassemia/mental retardation syndrome X- linked), leading to alternative lengthening of telomeres (ALT) without increase in telomerase activity. Ependymal tumors constitute a heterogeneous group of neoplasms seen both in children and adults, and found in various locations in the central nervous system. We analyzed the telomere maintenance mechanism of ependymal tumors and assessed its association with tumor recurrence.

Design: We reviewed all ependymal tumors including ependymomas (EP), anaplastic ependymomas (AEP), myxopapillary ependymomas (MPE) and subependymomas (SEP) diagnosed at UCSF between January 2004 and December 2013 and reached a consensus diagnosis. Cases without sufficient tissue, outside consultations, and tumor recurrences were excluded from molecular analyses. The *TERT* promoter region was analyzed by Sanger sequencing and tumors were classified as *TERT*-wild type and *TERT*-mutated. We used tissue micro arrays containing duplicate cores (2 mm) to assess ATRX status by immunohistochemistry.

Results: Ninety-six adults (45.7 +/- 15.8 years) and 22 children (8.3 +/- 6.3 years) with ependymal tumors were included in the study. All tumors retained their ATRX expression. All pediatric tumors (1 SEP, 6 EP, 15 AEP) were *TERT*-wild type, while seven adult tumors were *TERT*-mutated. One of 12 SEPs was TERT-mutated. Three MPEs were TERT-mutated, and two had recurred. This was higher than the recurrence rate of TERT-wild type MPE (1 out of 17, p=0.046). Three EPs were TERT-mutated, and two had recurred at 23 and 39 months. This was higher than the recurrence rate for TERT-wild type EP but did not reach statistical significance (11 out of 62, p=0.099).

Conclusions: TERT promoter mutations are seen in only a portion of ependymal tumors, and may be associated with higher recurrence rate. Given the low mutation frequency, larger multi-institutional studies are necessary. ATRX mutations were not identified in this cohort, arguing against ALT as a telomere maintenance mechanism in ependymal tumors. The mechanism of telomere maintenance in the majority of the ependymal tumors remains unknown and warrants further study.

1742 Clinical Implementation of Integrated Whole Genome Copy-Number and Mutation Profiling for Glioblastoma

Shakti Ramkissoon, Wenya Bi, Steven Schumacher, Lori Ramkissoon, Sam Haidar, David Knoff, Adrian Dubuc, Loreal Brown, Malak Abedalthagafi, David Reardon, Ian Dunn, Sandro Santagata, Rebecca Folkerth, Patrick Wen, Azra Ligon, Brian Alexander, Rameen Beroukhim, Keith Ligon. Brigham & Women's Hospital, Boston, MA; Dana-Farber Cancer Institute, Boston, MA.

Background: Multi-dimensional genotyping of formalin-fixed paraffin-embedded (FFPE) samples has the potential to improve diagnostics and clinical trials for brain tumors, but prospective use in the clinical setting is not yet routine. We report our experience with implementing a multiplexed copy-number and mutation-testing program in a CLIA-certified diagnostic laboratory.

Design: We collected and analyzed clinical testing results from whole genome array comparative genomic hybridization (OncoCopy) of 420 primary brain tumors, including 148 glioblastomas (GBMs). Targeted mass spectrometry-based mutation genotyping (OncoMap, 471 mutations) was generated on 86 GBMs.

Results: OncoCopy was successful in 99% of samples for which sufficient DNA was obtained (n=415). All characteristic aberrations of clinically relevant loci for gliomas and GBM were detected including *EGFR* and *PDGFRA* amplification, as well as *EGFRvIII*, *PTEN* deletion and 1p/19q co-deletion. Copy-number analysis in GBM patients $\leq$40 years old showed distinct profiles compared to those >40 years. OncoMap testing of GBMs identified recurrent mutations in *IDH1*, *TP53*, and *PTEN*. Integration of results from both platforms identified patients with complete tumor suppressor gene (TSG) inactivation but the frequency of this scenario was expectedly low (5%) due to lack of full gene coverage in OncoMap.

Conclusions: Combined use of multiplexed copy-number and mutation detection from FFPE samples in the clinical setting can efficiently replace singleton tests and provide extensive data for exploratory analyses and clinical trial screening. Limited capture of TSG variants reaffirms the need for whole gene sequencing in GBM.

1743 Molecular Categorization of Glioblastomas Using Next Generation Sequencing

Hope Richard, Jason Harrison, Catherine Dumur, Christine Fuller. Virginia Commonwealth University Health System, Richmond, VA.

Background: The prognosis of high-grade gliomas is poor with an average length of survival (LOS) of 18 months despite aggressive treatment. Therapeutic stratification of glioblastoma (GBM) patients is complicated by a recognized dichotomy of clinical outcomes in tumors that are histologically similar. Integrated genomic analysis has characterized GBMs into clinically relevant subtypes; however, molecular phenotyping of gliomas in the clinical arena remains sparse. Next generation sequencing (NGS) techniques have been recently developed that can utilize small amounts of DNA from formalin fixed paraffin embedded (FFPE), making them more practical in the clinical setting. The purpose of this study is to evaluate the utility of NGS as a clinical tool to augment the current prognostic indices for GBM and the development of potential molecular stratification for use in tumor specific therapies.

Design: DNA was extracted from FFPE tissue of 20 GBMs with varying LOS. Libraries for each were generated from 10 ng of dsDNA using the Ion AmpliSeq™ Cancer Hotspot Panel v2. The libraries were barcoded using the Ion Xpress™ Barcode Adapters kit and multiplexed in 10 samples per chip to achieve a 900X average depth-of-coverage. Sequencing was performed on the Ion Torrent PGM instrument with Ion 316™ chips. Results were aligned to the human genome reference sequence and identification of variants was ascertained using the variantCaller plugin 4.0. Clinical significance was performed by querying: COSMIC, dbSNP and ClinVAR. PolyPhen-2 algorithm predicted impact of amino acid substitution in missense mutations. Statistical significance was determined byFisher's exact test.

Results: Patients were stratified into two groups based on LOS (> or <18 months). Tumors from patients surviving <18 months showed a greater number of genes with mutations annotated as pathogenic when compared to the profile of tumors from patients with survival >18 months (12 vs. 8). Additionally, several genes showed a greater proportion of pathogenic mutations between the two groups; mutations in *AKT1*, *ALK*, *BRAF*, *CDH1*, *FGFR2*, *KIT*, and *PIK3A* were more likely to be mutated in tumors from patients surviving <18months.

Conclusions: NGS provides an efficient mechanism for GBM mutation analysis in the clinical arena. Multiple genes were noted to be associated with survival <18 months, several of which are drug targetable. Larger sample size is needed to identify statistically significant differences.

1744 Protein Expression of Angiogenesis Markers in the Prognosis of Human Gliomas

Hope Richard, Jason Harrison, Nathan Ardanowski, Christine Fuller, William Broaddus. Virginia Commonwealth University Health System, Richmond, VA; Virginia Commonwealth University, Richmond, VA.

Background: Vascular proliferation is an important factor in the progression of many tumor types including human gliomas. Hypoxia is important in the induction of angiogenic pathways, as are certain genetic anomalies. Numerous markers have been linked to this process including hypoxia inducible factor-1 (HIF1a) and CD31. This study aims to determine the incidence of CD31and HIF1a protein expression in human gliomas, with additional correlations sought regarding clinicopathologic parameters and patient outcomes.

Design: WHO grade I-IV tumors with adequate tissue and clinical follow-up were included. Pilocytic astrocytoma (16), subependymal giant cell astrocytoma (2), pleomorphic xanthoastrocytoma (1), low grade oligodendroglial tumor (11), anaplastic astrocytoma/oligodendroglial tumor (20), and glioblastoma (40) were all included in this study. Tissue microarrays (TMA) containing duplicate1 mm cores were generated from 90 gliomas (WHO grade I-IV) using an automated TMA system. Immunohistochemistry (IHC) was performed per the manufacture's recommendations. Samples with moderate (+1) or intense (+2) cytoplasmic staining with a polyclonal antibody to HIF1a (Novus) and CD31 (DAKO) were considered positive. Correlations were sought between intensity of staining, tumor pathology, length of overall survival (LOS) and progression free survival (PFS). Statistical analysis was performed using the Prism software package (one way ANOVA).

Results: 43% of the gliomas (WHO grade I-IV) evaluated showed moderate (35%) to intense (8%) staining for CD31. LOS correlated inversely with intensity of staining. The average LOS in tumors negative for CD31 (1499 days) was significantly longer than those with moderate (+1) or intense (2+) staining (600 and 473 days) (p= 0.0031). Similarly, when only high-grade gliomas were evaluated the average LOS for CD31 negative tumors (1145 days) was significantly longer than those with 1+ or 2+ staining (511 and 318 days) (p=0.0286). PFS was also significantly different in the two groups (p=0.0065). Additionally, 14% of the gliomas tested showed moderate or intense staining for HIF1a. No significant difference in overall or PFS was identified with HIF1a staining.

Conclusions: CD31 protein expression is associated with decreased overall and progression free survival in gliomas (WHO grade I-IV) tested. This difference is particularly pronounced in high-grade lesions.

1745 Immunohistochemical Study of Association Between Estrogen Receptor (ER) Status, Histone Modification Marks, and Survival in Uveal Melanoma (UM)

Lynn Schoenfield, Mary Aronow, Paula Carver, Raymond Tubbs, Yogen Saunthararajah, Arun Singh. Ohio State University Wexner Medical Center, Columbus, OH; Johns Hopkins Hospital, Baltimore, OH; Cleveland Clinic, Cleveland, OH.

Background: Aberrant histone modification patterns measured at the level of single nuclei have been shown to be predictive of cancer recurrence and poorer survival in multiple cancers. We previously reported that lower global levels of H3K4me1 measured by immunohistochemistry are associated with death by metastases and further that patterns of histone modification (H3K4me1 reduced/H3K9 elevated) suggest an aggressive phenotype in UM. We also previously found that ER is present in 48% of cases of enucleated melanomas. There is evidence to suggest that hormones modulate HDAC (histone deacetylase) expression in endometriosis, and hypoacetylation of H3/H4 within the promoter regions of the ERa gene has been demonstrated. We undertook to look for associations between ER and the histone modification marks and impact on clinical outcome.

Design: 32 cases of UM from 2004-10 treated by enucleation were stained by immunohistochemistry with a red chromagen for ER, H3K4me1 and H3K9. ER was considered positive if ≥ 1% of nuclei stained. H3K4me1 was considered reduced if ≤ 50% of nuclei stained, and H3K9 was considered elevated if ≥ 20% of nuclei stained. The results were compared to clinical outcome (DOD or metastasis) or presence of monosomy 3 (or 3p26 deletion) by FISH or SNP array (referred to as poor prognosis group).

Results: There were 20 men (63%) and 12 women (37%). 22 (69%) were in the poor prognosis group. ER was positive in 19 (59%) of cases, 16 (84%) of these being in the poor prognosis group. ER was negative in 13 (41 %) of cases, 6 (46 %) of which were in the poor prognosis group. 17 of the 32 (53%) showed the immunohistochemical pattern of an aggressive phenotype (H3K4 me reduced/H3K9 elevated). Of these 17 cases, 12 (71%) were positive for ER and of these 12 cases, 10 (83%) were in the poor prognosis group and the other 2 patients (17%) were alive without metastasis or monosomy 3 (good prognosis group). Of the 5 cases with the aggressive histone aggressive phenotype which were ER negative, 4 were in the poor prognosis group and 1 was not.

Conclusions: The interplay of histone modifications and the presence of ER in UM may warrant further study because these molecular pathways may prove amenable to therapies that already exist.

1746 Cytomegalovirus Is not Detected in Glioblastoma By Immunohistochemistry

Isaac Solomon, Shakti Ramkissoon, Danny Milner, Rebecca Folkerth. Brigham & Women's Hospital, Boston, MA.

Background: Glioblastoma (GBM), the most common and fatal primary brain tumor in adults, has seen minimal improvement in prognosis despite significant advances in characterizing its underlying genetic and molecular mechanisms. Recent studies have proposed a role for cytomegalovirus (CMV) in GBM pathogenesis, yet considerable debate remains over the validity of CMV as a therapeutic target. The reported rates of viral infection in tumor cells are widely discrepant, and prospective clinical trials with antiviral treatment have failed to show improved survival. However, subsequent retrospective analyses claiming an overall survival benefit have gained considerable publicity, prompting patients and neuro-oncologists to request CMV testing to justify antiviral treatment.

Design: To test for the presence of CMV infection in our GBM patient population, a tissue microarray (TMA) containing samples of 67 tumors was stained with anti-CMV antibody (DDG9/CCH2, DAKO, Carpinteria, CA) along with brain and non-brain controls. Tumor CMV IHC staining was correlated with information from patient records including age, gender, overall survival, CMV serology and viral titres, and features from the neuropathology report including MGMT promoter methylation, IDH1 (R132H) IHC, and gene copy number variation by array-based comparative genomic hybridization (aCGH).

Results: The patients in this study are 35 males and 32 females, with average age of 58.5 years at diagnosis, and median survival of 18 months. CMV serology was unavailable for all patients, and viral titres were negative (0/1 serum, 0/1 CSF). IDH1 (R132H) mutation and MGMT methylation were positive in 4/61 (6.7%) and 34/62 (54%) of tumors, respectively. aCGH analysis of 48 tumors showed polysomy 7 (CDK6, MET, and BRAF; 75%), PDGFRA gain (19%), and losses of CDKN2A (52%), PTEN (71%), RB1 (21%), NF1 (8%), TP53 (4%), and NF2 (21%). EGFR amplification was detected in 46/66 (70%) of cases by aCGH and/or *in situ* hybridization. IHC staining of the GBM TMA with anti-CMV antibody resulted in 0/67 positive cases (controls showed appropriate staining), thus no correlations could be drawn between CMV+ and CMV- IHC groups and any of the other variables.

Conclusions: Despite using optimized IHC protocols, 0/67 GBMs in this study stained positive for CMV. Therefore, these tumors either: 1) are not infected with CMV or 2) express CMV antigen below the level of detection of our clinical IHC laboratory. Taken together with the lack of proven efficacy of antiviral adjuvant therapy, we conclude that there is insufficient evidence at this time to recommend routine testing and treatment of CMV.

1747 Targeted Next Generation Sequencing of Uveal Melanoma Reveals Mutually Exclusive GNAQ and GNA11 Mutations

James Solomon, John Thorson, Jonathan Lin. University of California, San Diego, La Jolla, CA.

Background: The most common intraocular malignancy in adults, uveal melanoma (UM) arises from melanocytes in the choroid, ciliary body, and iris of the eye. Treatment of the primary tumor with enucleation and brachytherapy is effective, but UM has a strong propensity to metastasize, and systemic treatments for metastatic disease are lacking. The clinical and molecular features of UM are distinct from those of cutaneous melanoma, as UM lacks the *BRAF* and *NRAS* mutations that activate the MAP kinase pathway. However, mutations in *GNAQ* and *GNA11* are often seen, suggesting an alternative way of MAP kinase activation. Therefore targeted molecular therapies for cutaneous melanomas, such as the B-raf inhibitor vemurafenib, are not effective in treating UM. Here, we assess the molecular landscape of UM using a novel next generation sequencing (NGS) cancer gene panel assay that targets 47 cancer gene "hotspots".

Design: Enucleation specimens from 10 patients were collected from a single institution. DNA was extracted from unstained tissue sections and submitted for targeted NGS using a cancer gene panel of 47 commonly mutated cancer genes, including *BRAF, GNA11, GNAQ, HRAS,* and *NRAS*. A custom bioinformatics analysis pipeline was employed, using vendor-supplied software as well as in-house designed scripts for variant identification and annotation. Silent variants and known benign mutations were removed, and the remaining mutations were classified as either clinically validated mutations or mutations of uncertain significance.
Results: In each of the individual UM cases, only one mutated gene was identified by NGS, either *GNAQ* or *GNA11*. Neither clinically validated mutations nor mutations of uncertain significance were discovered in the hotspots of any of the other genes in the panel. In *GNAQ*, p.Q209L(c.626A>T) and p.Q209P(c.626A>C) mutations were identified, and in *GNA11*, p.Q209L(c.626A>T) mutations were seen.
Conclusions: The proteins encoded by *GNAQ* and *GNA11* are subunits of G-proteins which mediate signals from activated transmembrane receptors along cellular signaling pathways. Q209 is located within the GTP binding site, and its mutation constitutively activates the protein. Our data show that mutations in *GNAQ* and *GNA11* in UM samples are mutually exclusive, suggesting that either is sufficient for UM tumorigenesis. These mutations are thought to be involved early in the pathogenesis of UM, and we demonstrate here that they target a highly conserved enzymatic residue in the GTPase domain, suggesting a relatively homogeneous mechanism of UM tumorigenesis.

1748 SOX10 Expression and Genetic Alterations Distinguish Pigmented Ciliary Adenocarcinomas or Adenomas From Uveal Melanomas

Aoi Sukeda, Taisuke Mori, Shigeki Sekine, Akiko Maeshima, Shigenobu Suzuki, Atsushi Ochiai. National Cancer Research Center Hospital, Tokyo, Japan; National Cancer Research Center Research Institute, Tokyo, Japan; National Hospital Institute, Tokyo Medical Center, Tokyo, Japan.
Background: An adenocarcinoma or adenoma of the pigmented ciliary epithelium (APCE) is an exceptionally rare eye tumor. The tumors are known to have epithelioid and glandular features and often have PAS-positive basement membranes. There are few reports of APCEs, which are negative for keratin and positive for melanocytic markers. Therefore, diagnosis can be challenging, especially the differential diagnosis considering uveal melanoma (UM). SOX10 is a transcription factor that is crucial for the specification and maturation of the neural crest, and a reliable marker for skin melanomas. However, there are no examinations of SOX10 expression in the human eye and eye tumors. In addition, there is no information about genetic alterations influencing the APCE.
Design: We collected formalin-fixed paraffin-embedded specimens of 4 APCEs and 11 UMs of eye enucleation cases. The expression of SOX10, cytokeratin (CK) AE1/AE3, CK CAM5.2, S100, Melan-A, HMB45, and MITF were immunohistochemically examined and correlated with background eye structure and tumors. We also analyzed the genetic alterations associated with the tumors in the *GNAQ*, *GNA11*, *BRAF*, and *NRAS* genes, each of which is involved in malignant melanomas.
Results: In all 4 APCEs and background pigmented epithelial cells in ciliary bodies, SOX10 was not expressed in the nuclei, but was diffusely expressed in all 11 UMs and in background choroidal cells. The expression patterns of cytokeratin and melanocytic markers were variable in both groups of tumors. A genetic alteration analysis identified *BRAF* V600E mutations in 3 (75%) of 4 APCEs, but in none of the 11 UMs. Moreover, either *GNAQ* or *GNA11* mutations were found in 10 (91%) of 11 UMs, but not in APCEs. On the other hand, *NRAS* mutations were not observed in any of the tumors examined.
Conclusions: These observations indicate that APCEs and UMs have distinct SOX10 expression patterns and genetic backgrounds. In particular, the present study determined the lack of SOX10 expression and a high frequency of activating *BRAF* V600E mutations, but no *GNAQ* or *GNA11* mutations in APCEs. In contrast, UMs were positive for SOX10, and either *GNAQ* or *GNA11*, but no *BRAF* V600E, mutations were found. No *NRAS* mutations were observed in any of the tumors.

1749 PD-L1, HIF-1α, and Gliosis in Melanoma Brain Metastases

Dimitri G Trembath, Stergios Moschos, Anna Snavely, Evan Bradler, Nana Nikolaishvilli-Feinberg, Bentley Midkiff, Jonette Werley, Michael Krauze, Ronald Hamilton. University of North Carolina, Chapel Hill, NC; University of Pittsburgh Medical Center, Pittsburgh, PA.
Background: Adjusted for incidence, melanoma has the highest propensity for CNS spread among solid tumors and is associated with worse prognosis than non-metastatic melanoma. High intratumoral hemorrhage and low/absent lymphocytic infiltrates are associated with shorter OS (time from craniotomy to death). Whole genome expression profiling showed the Biocarta pathway "Hypoxia-inducible factor (HIF)" was associated with worse OS. Intratumoral hemorrhage and the HIFα pathway can be related to angiogenic cytokine dysregulation and/or blood vessel density/maturation (BV).This discovery, coupled with our finding of lymphocytic infiltrates in MBM, led us to study PD-L1, angiogenic/hypoxic factors, and BV quality/density in MBM.
Design: MBM samples were stained by IHC for angiogenic/hypoxic factors (bFGF, VEGF, HIF1α), BV density (CD31), and PD-L1. BV was also defined by immunofluorescence as mature or immature blood vessels based on expression of smooth muscle actin (SMA; MBV, CD31+SMA+; IBV, CD31+SMA-). Images from scanned slides were 'segmented' into compartments for melanoma, gliosis, normal brain, and inflammation. The Aperio system and Definiens Tissue Studio were used to analyze expression (H-score) of each marker/compartment. For detection/quantification of non-capillary blood vessels we used Definiens Architect software with Tissue Studio portal. For statistical analysis, OS information was used to define the optimal cut-point in H-score between high and low expression of each marker. Survival analysis was performed to determine the association between each marker, treated as a dichotomous variable.
Results: An average of 44 cases were analyzed for each stain. When survival information was used to define the optimal cut-point for each variable between cases with long versus short OS, high tumor expression of PD-L1 and bFGF and low tumor expression of HIF1α were associated with worse OS (unadjusted $p < 0.05$; hazard ratios 1.92, 2.2, and 2.1 respectively). HIF1α and bFGF expression were significantly higher in tumor compared to gliosis. Neither the quality nor density of blood vessels was significant.
Conclusions: Immune suppression within the brain, as reflected by PD-L1, is an adverse prognostic factor. Gliosis appears to contribute equally towards this event, along with metastatic tumor. The favorable prognostic significance of tumor HIF1α expression is additional evidence that peritumoral edema may not be an adverse indicator in brain metastases. Future work will include analysis of angiopoeitin-2 and galectin-9, markers of angiogenesis and immune checkpoints.

1750 Comparative Analysis of STAT6 Immunoexpression and NAB2-STAT6 Gene Fusion Types in 58 Meningeal Solitary Fibrous Tumors/Hemangiopericytomas

Jen-Wei Tsai, Shih-Ming Jung, Chien-Feng Li, Shih-Chiang Huang, Hui-Chun Tai, Yu-Chien Kao, Jui Lan, Hsuan-Ying Huang. E-DA hospital, Kaohsiung, Taiwan; Chang Gung Memorial Hospital and Chang Gung University College of Medicine, Taoyuan, Taiwan; Chi Mei Medical Center, Tainan, Taiwan; Kaohsiung Chang Gung Memorial Hospital and Chang Gung University College of Medicine, Kaohsiung, Taiwan; Changhua Christian Hospital, Changhua, Taiwan; Wan Fang Hospital and Taipei Medical University, Taipei, Taiwan.
Background: There exist conflicting viewpoints in tumor classification about unifying or separating solitary fibrous tumors (SFT) and hemangiopericytomas (HPC) of the meninges. Recent genetic breakthrough indicates that meningeal tumors exhibiting either histological pattern harbor the same inv(12)(q13q13)-derived *NAB2-STAT6* fusion as the somatic SFTs have. However, the prevalence rates of various *NAB2-STAT6* types and STAT6 immunoexpression and localization in meningeal SFT/HPCs remain under-characterized.
Design: We retrospectively retrieved 58 memingeal SFT/HPCs to review clincopathological features, assess the immunoexpression of STAT6, and determine *NAB2-STAT6* fusion variants by RT-PCR and Sanger sequencing.
Results: There were 33 males and 25 females aged between 16 and 85 years (median, 43), who received surgical excision for 53 intracranial and 5 spinal tumors with a median size of 4.6 cm (range, 1.2~14.5). Based on the mitosis ≥ 4/10 HPFs with necrosis and/or nuclear pleomorphism, histological malignancy was recognized in 6 of 42 cellular tumors classified as HPCs and in 2 of 16 SFTs with ropy collagen fibers. Regardless of histological patterns, distinctive nuclear STAT6 expression was found in the vast majority (96%) and strongly and diffusely stained in 44 of SFT/HPCs (75%) but not in any meningioma tested. RT-PCR assay on formalin-fixed samples successfully detected fusion variants of *NAB2ex6-STAT6ex16/17 in 17 (81%), NAB2ex4-STAT6ex2/3 in 3 (14.3%), and NAB2ex7-STAT6ex2 in 1 (4.7%). Twenty-seven cases developed local recurrences and 7 had liver or bone metastases, with 5 dead of tumors. The inferior disease-free survival was marginally related to mitosis* ≥ 4/10 HPFs (p=0.067) but unrelated to fusion variants or STAT6 immunoexpression.
Conclusions: Immunostain demonstrating STAT6 nuclear relocation is a diagnostic alternative of detecting *NAB2-STAT6* transcript in meningeal SFT/HPC, most of which harbor the predominant *NAB2ex6-STAT6ex16/17* variant that appears unrelated to clinical behavior.

1751 The Immunophenotype of the Sarcomatous Components of Gliosarcomas: Emphasis on the Expression of CD10

Jose Velazquez Vega, Carol Petito, Mehrdad Nadji. University of Miami, Jackson Memorial Hospital, Miami, FL.
Background: Gliosarcoma is an uncommon malignant central nervous system tumor characterized by a biphasic pattern comprised of malignant glial and sarcomatous components. As defined by the WHO Classification, it represents a glioblastoma (GBM) variant and, as such, corresponds to a WHO grade IV tumor. The sarcoma components of these neoplasms have been described to be fibrosarcoma, or to differentiate along other mesenchymal lines. In this study, we evaluated the immunohistochemical phenotype of gliosarcomas with special emphasis on expression of CD10 in the sarcomatous elements. We hypothesized that CD10, a metalloendoprotease, may be expressed in these neoplasms as it has been described in close to 50% of soft tissue sarcomas.
Design: The cases were selected from the files of the Department of Pathology at the University of Miami / Jackson Memorial Hospital and the histologic diagnoses of gliosarcoma were confirmed. Immunohistochemistry was performed for GFAP, desmin, wide-spectrum keratin, S100 protein, SMA, CD34 and CD10.
Results: The study included eight cases from seven patients with primary gliosarcoma and one patient with prior diagnosis of GBM and subsequent recurrence as post-radiation gliosarcoma. All gliosarcomas showed a biphasic pattern in which the sarcomatous components were comprised of neoplastic spindle cells interlaced with glial elements. In all cases, the sarcomatous component was negative for GFAP and positive for CD10, with strong membrane and cytoplasmic staining. The glial components were universally negative for CD10. SMA was variably positive in the sarcomatous areas of all cases and in the glial component of 50% of the cases. In three tumors, the CD10 and SMA positivity were more prominent in areas of microvascular proliferation with glomeruloid formations. The expression of markers in each component of gliosarcomas is summarized in the table.

Component	GFAP	S100	Keratin	Desmin	SMA	CD34	CD10
Glial	100%	100%	0%	62%	50%	62%	0%
Sarcomatous	0%	12.5%	0%	50%	100%	0%	100%

Conclusions: To our knowledge, this study represents the first to describe CD10 expression in gliosarcomas. While negative in the glial components, CD10 always was positive in the sarcomatous components. Therefore, CD10 may be a useful marker for histologic delineation of sarcomatous elements of gliosarcomas. Whether or not CD10 plays a biologic role in gliosarcomas, akin to that in a number of other malignant neoplasms, remains to be elucidated.

1752 Immunohistochemical and Gene Expression Analysis of Recurrent Glioblastoma Shows Increased Expression of Mesenchymal Markers on Tumor Recurrence

Matthew Wood, Gerald Reis, Joanna Phillips. University of California, San Francisco, CA.

Background: Glioblastoma (astrocytoma, WHO grade IV) is characterized by molecular heterogeneity, near universal tumor recurrence, and a poor clinical outcome despite the use of multiple therapeutic modalities. The stability of glioblastoma molecular traits on recurrence is only partly characterized, and additional data are needed to guide treatment of recurrent disease and to identify drivers of heterogeneity in recurrent tumors.

Design: We generated tissue microarrays of paired primary and recurrent glioblastoma specimens (N = 21 pairs) for immunohistochemical (IHC) analysis, and simultaneously extracted messenger RNA (mRNA) from a subset of paired tumors to correlate gene expression changes with IHC findings. Messenger RNA levels for a panel of 173 genes were assessed using Nanostring technology. The IHC markers included Ki67, CD34, phosphorylated S6 kinase (pS6K), YKL40, phosphorylated STAT3 (pSTAT3), CD44, OLIG2, EGFR, and IDH1^{R132H}. Protein expression levels on IHC were scored on a 3-unit semi-quantitative scale; CD44 was scored on a 6-unit scale.

Results: Recurrent glioblastoma showed a significant increase in protein expression of the mesenchymal marker CD44 (4.34 versus 3.42 units, $p < 0.043$), which was accompanied by an increase in CD44 mRNA ($p < 0.028$) and reduced mRNA levels of the proneural marker OLIG2 ($p < 0.004$). Primary tumors with low protein expression of mesenchymal markers CD44, YKL40 or pSTAT3 showed increased expression of these markers on tumor recurrence (mean increase 2.7 units [$p < 0.0001$], 0.41 units [$p < 0.0136$], and 0.89 units [$p < 0.0058$], respectively). Primary tumors with high protein expression of CD44 and YKL40 showed persistently high expression on recurrence. Conversely, primary tumors with high protein expression OLIG2 showed reduced OLIG2 expression on tumor recurrence (mean decrease 1.57 units, $p < 0.0214$), while primary tumors with low OLIG2 levels showed no significant change on recurrence.

Conclusions: Recurrent glioblastoma showed increased expression of markers associated with a mesenchymal phenotype by both gene expression and immunohistochemical analysis. The mechanisms driving this process may give insight into the molecular evolution of glioblastoma in response to treatment.

1753 Discarded Casette Content From Routine Vitrectomies Includes Tissue That Provide Valuable Information in Diabetic Patients

Pablo Zoroquiain, Sarah Alghamdi, Natalia Vila, Vasco Bravo-Filho, Patrick Logan, Michael Kapusta, John Chen, Miguel Burnier. McGill University, Montreal, QC, Canada.

Background: Diabetic retinopathy is a clinical diagnosis made by fundus examination. When it comes to diabetes progression, it is not possible to obtain a biopsy in the eye where the risks are higher than the benefits. Our purpose is to describe the histopathological features of vitreous samples from diabetic patients.

Design: Vitreous specimens from 137 patients who underwent pars planavitrectomy for different clinical conditions were analyzed.All samples were centrifuged and the resulting pellet from each sample was fixed in a 1:1 alcohol and formalin solution. The supernatant was discarded and sediment was processed as part of routine paraffin section histopathology. The sample characteristics, cell type and vascular findings were evaluated and categorized (0=negative; 1=low; 2=high). When vessels were recorded, the presence of pericytes was evaluated by alpha-SMA(aSMA), and was semiquantified as total loss (3), >50% (2), <50% (1) and no loss (0). The results were compared between diabetic and non-diabetic patients.

Results: Of the 137 patients included only 12 samples were excluded in this study due to scant material. Of the 125 included(58 diabetic, 67 non-diabetic), 75 were male. The mean age of included patients was 64.2+14 years. The presence of haemorrhage, inflammatory cells and histiocytes were significantly higher in the diabetic group than the non-diabetic group (P=0.001; P=0.028; P=0.016 respectively). Moreover, the diabetic group had significantly more vessels (P=0.001) and ghost vessels (P=0.049). All non diabetic cases had a 0 aSMA score while all diabetic ones showed pericyte loss (>1 score).

Conclusions: In this study, we found different histopathological features in vitreous samples from diabetic and non-diabetic patients. The presence of haemorrhage, histiocytes, vessels and ghost vessels were associated with a diagnosis of diabetes. Analysis of vitreous cytology may serve as a diagnostic tool for clinically undetectable diabetic retinopathy. In addition, this technique may be used to evaluate diabetic retinopathy-like damage in glucose intolerant patients.

Pancreas and Biliary Tree

1754 Gallbladder Carcinomas With Sarcomatoid Component: Clinicopathologic Analysis of 11 Cases

Gizem Akkas, Bahar Memis, Pelin Bagci, Nevra Dursun, Burcu Saka, Olca Basturk, Kee-Taek Jang, Juan Roa, Juan Sarmiento, Volkan Adsay. EU, Atlanta, GA; Wayne State University, Detroit, MI; SMC, Seoul, Korea; PCU, Santiago, Chile.

Background: Sarcomatoid differentiation is uncommon in gallbladder carcinomas (GBC), and data on the clinicopathologic characteristics of GBCs with a sarcomatoid component is highly limited.

Design: Among 656 GBCs, 11 cases with a sarcomatoid component constituting ³25% of the tumor were identified. Their clinicopathologic characteristics were analyzed/ contrasted with those of ordinary GBC (O-GBC).

Results: The patients were 9 female, 2 male (F/M=4.5, vs 3.9 in O-GBC). Mean age was 71 yr (vs 64). Mean and median tumor sizes were 5.3 and 4.6 cm (vs 2.9 and 2.5, respectively; P=0.01). Nine patients (84%) presented with advanced stage (pT3/4) tumors (vs 48%). Of 7 known, 6 had gallstones. Microscopically, an adenocarcinoma component was present in 9, constituting 1-75% of the tumor, and 8 had surface dysplasia/CIS. An intracholecystic papillary tubular neoplasm was identified in 1. Seven revealed pleomorphic-sarcomatoid pattern (as defined in the upper aerodigestive tract), 4 showed prominent spindle cell pattern composed of subtle, bland, stromal-appearing cells, and 1 was mistaken as granulation tissue on frozen section. Three cases had angiosarcomatoid pattern with prominent clefts and/or intermixed vascularity with RBCs. Two cases had heterologous elements (1 bone/cartilage, 1 cartilage only). Only 1 showed focal osteoclast-like giant cells. Lymph node metastasis was present in 2/5. Immunohistochemically, vimentin was (+) in 6/6, epithelial markers were retained in the sarcomatoid components of most (AE1/AE3 6/7, CK18 5/6, and EMA in 5/6) along with at least focal expression of MUC1 (5/6). p63 was (+) in 2/6. Actin, desmin and S100 were negative in all (0/6). Median Ki67 index was 40%. P53 expression was >60% in 6/6. MLH1 and MSH2 were retained. One patient died peri-operatively. Of the remaining 10, 8 died of disease within 3 to 8 mos, and 2 were alive at 9 and 15 mos (vs median survival of 26 mos for O-GBC).

Conclusions: Sarcomatoid undifferentiated component is seen in <2% of GBC. It typically occurs in the company of ordinary adenocarcinoma. Unlike the ones in the remainder of pancretobiliary tract, these are seldom of "osteoclastic" type. Also, in contrast with the sarcomatoid carcinomas of other sites, these often retain keratin positivity. The patients present with large/advanced-stage tumors that have high proliferation index. Limited data suggests that these tumors are highly aggressive with rapid mortality.

1755 Pathologic Diagnosis as the Reason for Wide Discrepancies in the Literature Regarding the Incidence and Behavior of T1 Gallbladder Cancer (GBC): An Analysis of 473 GBC and Comparison With Literature

Gizem Akkas, Bahar Memis, Olca Basturk, Brian Quigley, Selda Karaaslan, Burcu Saka, Nevra Dursun, Pelin Bagci, Serdar Balci, Juan Sarmiento, Sudeshna Bandyopadhyay, Oscar Escalona, Michael Goodman, Jessica Knight, Alyssa Krasinskas, Juan Roa, Volkan Adsay. EU, Atlanta, GA; Wayne State University, Detroit, MI; PUC, Santiago, Chile.

Background: For T1 GBC, there is highly conflicting data on both its relative frequency among invasive ca (20–44%) and prognosis (5-yr, ~90% in Korea/Japan, where cholecystectomy is regarded curative, vs< 50%in the SEER/West-Other, with radical operations performed).

Design: 473 in-situ and invasive GBC (248 from Chile, 225, US) were carefully re-analyzed.

Results: 124 were determined to be Tis (non-invasive) and 349 invasive. See table for T-stage distribution of invasive ones.

	PT1	PT2	PT3	TOTAL
USA	7	81	115	203
CHILI	14	84	48	146

USA: Only 10 had been reported as T1,3 of which proved to be T2. Chile: Of the 51 cases that had been classified as "early GBC" (Tis/T1), 4 was upstaged to T2 and only 14 showed definitive T1 by the Western criteria. Of the 26 T1 cases (including 5 consultation cases not included in the frequency analysis), 2 died perioperatively, 2 died of GBC at 6 and 27 mos, 3 died of other causes, 2 were lost to follow up, and the remaining 17 were alive without disease at a median of 110mos (over all 5-year survival, 67%; disease-specific survival, 91%).

Conclusions: In Chile, where it has been managed as a major healthcare problem, GBCs are detected in earlier stages (Tis + T1 constituting 47% of the cases, vs 12%in the US). **I.** With careful pathologic examination and invasiveness criteria employed in the West,< 10% of invasive GBCs qualify as T1 (US,3%, Chile 9%), which is not surprising considering T1 of GBC essentially corresponds to "intramucosal adenoca" of other sites because of the mucosal thinness, and the tunica muscularis acting like muscularis-mucosa. **II.** Markedly higher frequency of T1 in the literature (SEER, 40%, Korea, 35%) is attributable to the pathologic over-staging of complex Tis cases as T1, which is also not surprising considering GB mucosa is often complex with florid glandular proliferations and invaginations with pseudoinvasive patterns. **III.** The behavior of T1 seems to be much better than reported in the West/SEER data(5-yr, 35-50%), which is attributable to under-staged T2s (in this study, 7 that had been reported as T1/EGBC were re-classified as T2). **IV.** Considering all these challenges/